CELL BIOLOGY

RIPK1 blocks T cell senescence mediated by RIPK3 and caspase-8

Takayuki Imanishi[1]*, Midori Unno[1], Natsumi Yoneda[1], Yasutaka Motomura[2,3,4], Miho Mochizuki[4], Takaharu Sasaki[5,6], Manolis Pasparakis[7], Takashi Saito[1,8]*

Receptor-interacting protein kinase 1 (RIPK1) regulates cell death and inflammation. Here, we show that T cell–specific RIPK1 deficiency in mice leads to the premature senescence of T cells and induces various age-related diseases, resulting in premature death. RIPK1 deficiency causes higher basal activation of mTORC1 (mechanistic target of rapamycin complex 1) that drives enhanced cytokine production, induction of senescence-related genes, and increased activation of caspase-3/7, which are restored by inhibition of mTORC1. Critically, normal aged T cells exhibit similar phenotypes and responses. Mechanistically, a combined deficiency of RIPK3 and caspase-8 inhibition restores the impaired proliferative responses; the elevated activation of Akt, mTORC1, extracellular signal–regulated kinase, and caspase-3/7; and the increased expression of senescence-related genes in RIPK1-deficient CD4 T cells. Last, we revealed that the senescent phenotype of RIPK1-deficient and aged CD4 T cells is restored in the normal tissue environment. Thus, we have clarified the function of RIPK3 and caspase-8 in inducing CD4 T cell senescence, which is modulated by environmental signals.

INTRODUCTION

Age-associated inflammation, called "inflammaging," is characterized by chronic, low-grade, systemic inflammation with aging in the absence of infection, which leads to tissue degeneration (*1*). Inflammaging is a risk factor for type 2 diabetes, cardiovascular diseases, neurodegenerative diseases, cancer, and death and leads to increased susceptibility to infection in the elderly (*2*).

Age-associated inflammation, called inflammaging, is characterized by chronic, low-grade, systemic inflammation with aging in the absence of infection, which leads to tissue degeneration (*1*). Inflammaging is a risk factor for type 2 diabetes, cardiovascular diseases, neurodegenerative diseases, cancer, and death and leads to increased susceptibility to infection in the elderly (*2*). Aging also induces thymic involution, which results in a decrease of naïve T cells and an accumulation of memory T cell subsets (*3*). The proliferative response of these senescent T cells upon T cell receptor (TCR) stimulation is impaired, leading to reduced vaccine efficacy and increased susceptibility to cancer and infections in elderly people (*3*, *4*). Senescent cells secrete high levels of inflammatory cytokines, chemokines, matrix metalloproteinases, growth factors, and angiogenic factors, termed the senescent-associated secretory phenotype (SASP) (*5*). The SASP factors contribute to inflammaging, contribute to induction of insulin resistance and fibrosis, and reinforce and propagate senescence by both autocrine and paracrine mechanisms (*5*). Thus, the SASP mediates many of the pathological effects by senescent cells. Mechanistically, the SASP is controlled by enhancer remodeling and activation of transcription factors, such as nuclear factor κB (NF-κB), CCAAT/enhancer binding protein β (C/EBPβ), and GATA binding protein 4 (GATA4), and by activation of mitogen-activating protein kinases (MAPKs) and mechanistic target of rapamycin (mTOR) (*5*).

The nutrient-sensing serine/threonine kinase mTOR integrates extracellular signals and intracellular metabolic cues and promotes glycolysis, growth, and proliferation. mTOR forms two distinct protein complexes, mTORC1 and mTORC2, and a deficiency of both complexes in T cells results in impaired T cell activation and differentiation (*6*, *7*). Optimal mTOR activity is required for proper T cell functions. T cell–specific deletion of Tuberous sclerosis 1 (TSC1), an upstream negative regulator of mTORC1, abrogates naïve T cell quiescence, increases apoptosis, and impairs antibacterial immune responses (*8*–*10*).

Recent studies revealed that dominant-active gain-of-function mutations in phosphatidylinositol 3-kinase (PI3K) result in hyperactivation of Akt and mTOR in T cells, leading to T cell senescence and immunodeficiency in humans (*11*). Senescent T cells also exhibit hyperactivation of MAPK cascades, which is mediated by a complex of MAPKs and stress-sensing proteins, sestrins (*12*). However, the molecular mechanisms of hyperactivation of mTOR and MAPKs in senescent T cells and the pathological role of senescent T cells remain unclear.

RIPK1 is a key signaling molecule controlling cell death and inflammation through both its scaffold and kinase functions (*13*, *14*). The kinase function of RIPK1 induces caspase-8–dependent apoptosis and RIPK3-dependent necroptosis (*15*–*18*). On the other hand, RIPK1 inhibits apoptosis and necroptosis through its scaffold function, which is critical for blocking early postnatal lethality mediated by caspase-8 and RIPK3 (*19*–*21*).

[1]Laboratory for Cell Signaling, RIKEN Center for Integrative Medical Sciences (IMS), Yokohama, Kanagawa 230-0045, Japan. [2]Laboratory for Innate Immune Systems, Department of Microbiology and Immunology, Graduate School of Medicine, Osaka University, Suita, Osaka, Japan. [3]Laboratory for Innate Immune Systems, Immunology Frontier Research Center, Osaka University, Osaka 565-0871, Japan. [4]Laboratory for Innate Immune Systems, RIKEN Center for Integrative Medical Sciences (IMS), Yokohama, Kanagawa 230-0045, Japan. [5]Laboratory for Intestinal Ecosystem, RIKEN Center for Integrative Medical Sciences (IMS), Yokohama, Kanagawa 230-0045, Japan. [6]Present address: Biomedical Research Core Facilities, Juntendo University Graduate School of Medicine, Tokyo 113-8421, Japan. [7]Institute for Genetics, Centre for Molecular Medicine (CMMC), and Cologne Excellence Cluster on Cellular Stress Responses in Aging-Associated Diseases (CECAD), University of Cologne, 50674 Cologne, Germany. [8]Laboratory for Cell Signaling, Immunology Frontier Research Center, Osaka University, Suita, Osaka 565-0871, Japan.
*Corresponding author. Email: takashi.saito@riken.jp (T.Sai.); takayuki.imanishi@riken.jp (T.I.)

Recent studies characterized a complete RIPK1 deficiency in patients with biallelic loss-of-function mutations in the *RIPK1* gene (*22*, *23*). The patients suffered from recurrent infections, early onset inflammatory bowel disease, and progressive polyarthritis (*22*, *23*). The patients had lymphopenia, suggesting the possibility of a functional importance of RIPK1 in T cells (*22*). Consistent with the human data, a recent study demonstrated that T cell–specific deletion of RIPK1 leads to severe T lymphopenia in mice, whereas the immature T cell compartment in the thymus was intact (*24*). Moreover, RIPK1-deficient [knockout (KO)] T cells were defective in TCR-induced proliferation and exhibited elevated caspase activation independently of kinase activity (*24*). However, whether RIPK1-KO in T cells results in immunodeficiency and inflammatory diseases remains unknown.

In this study, we found that T cell–specific RIPK1 deficiency leads to the premature senescence in T cells, which is accompanied by the SASP. T cell–specific RIPK1-KO (tKO) mice develop chronic inflammatory diseases with aging, resulting in premature death. We demonstrate that basal activation of Akt, mTORC1, and extracellular signal–regulated kinase (ERK) is enhanced in RIPK1-KO T cells and that inhibition of both RIPK3 and caspace-8 or mTORC1 inhibits T cell senescence, SASP, and caspase-3/7 activation. These basal activation phenotypes were similarly observed in aged wild-type (WT) T cells. We further demonstrated that the senescent phenotype of aged and RIPK1-KO CD4 T cells is restored in the normal tissue environment.

RESULTS

RIPK1 deficiency in T cells induces inflammatory diseases

To elucidate the physiological functions of RIPK1 in T cells, we specifically deleted *Ripk1* in T cells by crossing *Ripk1*$^{fl/fl}$ mice with CD4-Cre Tg mice (designated as RIPK1-tKO). Consistent with a previous report (*24*), RIPK1-tKO mice look normal until 4 months of age. However, they develop inflammatory diseases characterized by a reduced body weight, eye opacity, and infiltration of leukocytes in the salivary gland and lung from 5 months of age (Fig. 1, A to F). We also observed an increased inflammatory cell infiltration in the bronchioalveolar lavage (BAL) of RIPK1-tKO mice (Fig. 1G). Despite these inflammatory manifestations, RIPK1-tKO mice showed no elevation of serum double-stranded DNA (dsDNA) autoantibody levels as representative of generalized autoimmunity (fig. S1A). RIPK1-tKO mice also showed hindlimb paralysis (Fig. 1, H and I), which was characterized by clenching of the hindlimbs to the body when suspended by the tail, a common neuropathic phenotype. Because axon abnormalities and subsequent degeneration of the sciatic nerve are common causes of hindlimb paralysis, the sciatic nerve morphology was examined. Semithin sections of sciatic nerve showed a remarkable decrease in myelinated axons and axon diameter in RIPK1-tKO mice compared to control mice (Fig. 1, J and K). Accordingly, the infiltration of leukocytes and the increased expression of Ifng, Cxcl10, and Cd3e were observed in the sciatic nerve of RIPK1-tKO mice (Fig. 1L). Last, RIPK1-tKO mice showed premature death; more than half of mice died by 8 months (Fig. 1M). These results demonstrated that RIPK1 deficiency in T cells causes multiorgan inflammation and eventually results in premature death.

RIPK1 deficiency causes premature CD4 T cell senescence

To understand how the RIPK1-tKO causes inflammatory diseases with aging, the cellularity of the spleen in young (2 to 4 months, apparently healthy) and middle-aged (6 to 10 months, already developed inflammatory diseases) RIPK1-tKO mice was first assessed. The total number of spleen cells was increased in middle-aged but not young RIPK1-tKO mice compared with control mice, whereas the numbers of both CD4 and CD8 T cells were markedly decreased in RIPK1-tKO mice (Fig 2A and fig. S2, A and B). Whereas the expression of RIPK1 in RIPK1 heterozygous CD4 T cells is half of WT CD4 T cells (fig. S2C), the number of CD4 and CD8 T cells in the spleen from RIPK1 heterozygous mice was comparable to that of WT mice (fig. S2D). The percentage and number of CD44^{hi} CD62L^{lo} effector/memory phenotype CD4 T cells markedly increased, whereas that of CD44^{lo} CD62L^{hi} naïve CD4 T cells inversely decreased in RIPK1-tKO mice with aging (Fig. 2, B and C, and fig. S2, E and F).

We next assessed the contribution of RIPK1-KO regulatory T cells (T_{regs}) to the inflammatory phenotype of RIPK1-tKO mice using T_{reg}-specific RIPK1-deficient mice by crossing RIPK1$^{fl/fl}$ mice with Foxp3YFP-Cre mice (designated as Foxp3cre RIPK1$^{fl/fl}$). Foxp3cre RIPK1$^{fl/fl}$ mice did not develop inflammatory diseases such as the eye opacity and hindlimb paralysis (fig. S2, G and H), indicating that the inflammatory phenotype of RIPK1-tKO mice was not attributed to the dysregulation of RIPK1-KO T_{regs}.

To identify the molecular mechanism by which RIPK1-KO T cells drive inflammation, we sorted CD4$^+$ CD25$^-$ T cells of the spleen from 10-month-old control or RIPK1-tKO mice (fig. S2I), and RNA sequencing (RNA-seq) analysis was performed. We found that the expression of *Spp1* encoding osteopontin, a marker of senescent CD4 T cells, was markedly up-regulated in RIPK1-KO CD4 T cells (Fig. 2D) (*25*, *26*), suggesting that RIPK1-KO T cells exhibit a cellular senescence phenotype. The expression of other cellular senescence and SASP-related genes represented by *Gzma/b/k*, *Adam8/9/19*, *Vegfb*, *Pdgfb*, *Ctsb/e*, *Ccl5*, *Il1r2*, *Prdm1*, and *Pdcd1* was also up-regulated in RIPK1-KO CD4 T cells (Fig. 2D and fig. S2J). The expression of genes encoding proinflammatory cytokines and chemokines (fig. S2J), proinflammatory transcriptional factors such as NF-κB and interferon (IFN) regulatory factors (fig. S2K), and cytokine and chemokine receptors (fig. S2L) was increased in RIPK1-KO CD4 T cells. RIPK1-KO CD4 T cells produced higher amounts of cytokines such as IFN-γ, interleukin-17A (IL-17A), IL-4, and IL-5, although their proliferative responses upon TCR stimulation were impaired (Fig. 2E). Thus, RIPK1-KO CD4 T cells functionally exhibit the characteristics of senescent T cells. We also analyzed the T cells from the lymph nodes in RIPK1-tKO mice and found that the expression of senescence-related genes was increased in CD4 T cells of the lymph nodes from RIPK1-tKO mice (fig. S2M). Next, the serum levels of inflammatory cytokines were examined, and the levels of IFN-γ, IL-2, IL-5, IL-17A, and tumor necrosis factor–α (TNF-α) were found to be increased in RIPK1-tKO mice (Fig. 2F). Similarly, the serum levels of immunoglobulin M (IgM), IgG, and IgE were also significantly enhanced in these mice (Fig. 2F). Notably, the serum levels of inflammatory cytokines except for IL-17A were increased even in young RIPK1-tKO mice that appear healthy. These data indicate that RIPK1-KO T cells induce chronic inflammation from an early age, resulting in premature inflammatory diseases in middle-aged RIPK1-tKO mice.

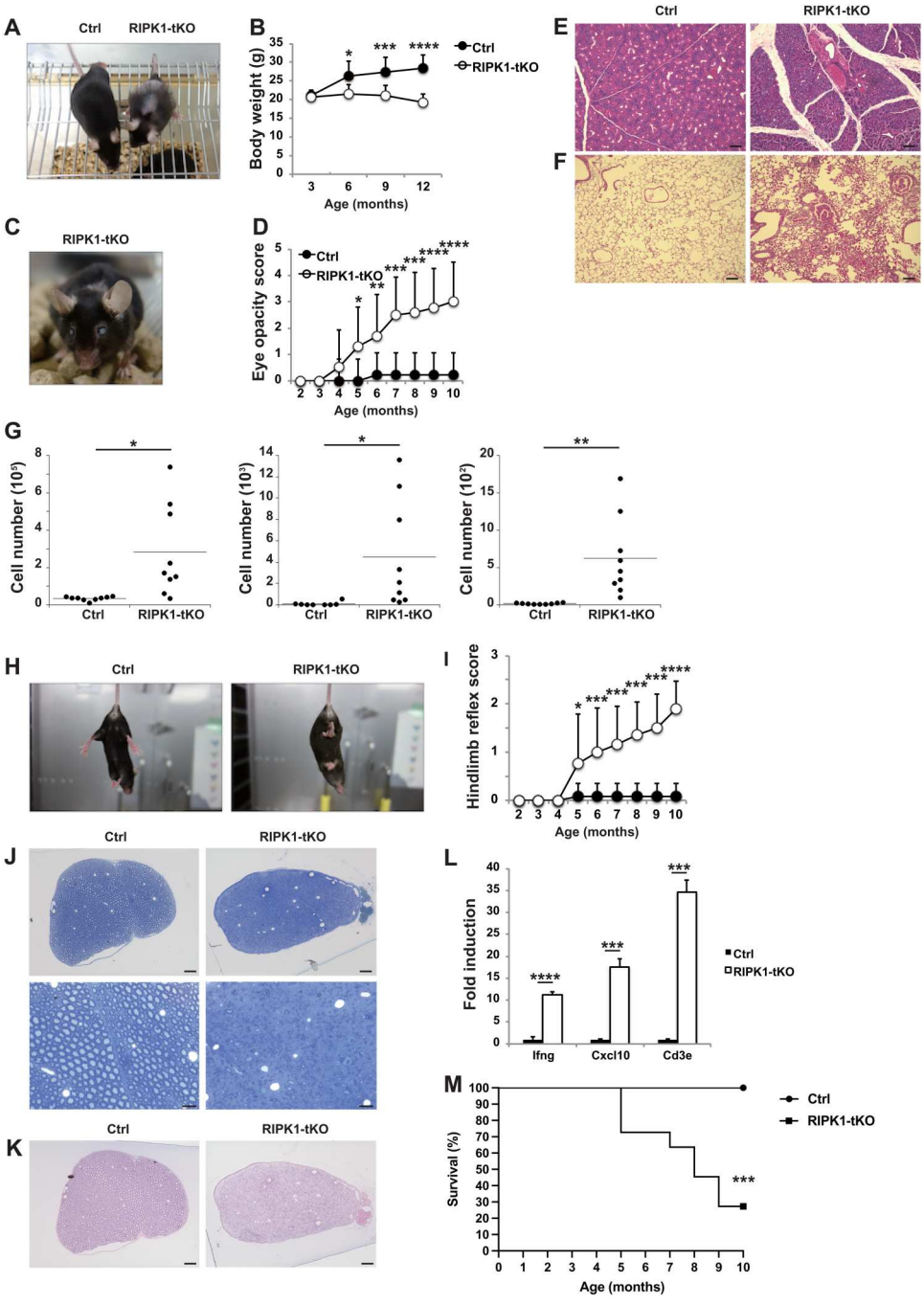

Fig. 1. RIPK1-tKO mice develop inflammatory disease. (**A**) Representative photograph showing the appearance of control and 10-month-old RIPK1-tKO mice (right). (**B**) Body weight changes over time in control ($n = 6$) and RIPK1-tKO female mice ($n = 8$). (**C**) Representative photograph of a 10-month-old RIPK1-tKO mouse that has developed opacity of the eyes. (**D**) Eye opacity score of control ($n = 10$) and RIPK1-tKO ($n = 13$) mice. Representative hematoxylin and eosin (H&E)–stained sections of salivary glands (**E**) and lung (**F**). Scale bars, 100 μm (E) and 50 μm (F). (**G**) Quantification of total cells (left), eosinophils (middle), and neutrophils (right) in the BAL fluid from 7- to 10-month-old control and RIPK1-tKO mice ($n = 9$ per group). (**H**) Representative photograph of 8-month-old control and RIPK1-tKO mice suspended by the tail. RIPK1-tKO mice clench their hindlimbs to the body. (**I**) Hindlimb reflex score of control and RIPK1-tKO mice ($n = 13$ per group). (**J**) Toluidine blue–stained semithin transverse sections of the sciatic nerve from 8-month-old control and RIPK1-tKO mice. Scale bars, 50 μm (top) and 20 μm (bottom). (**K**) H&E-stained semithin transverse sections of the sciatic nerve from 8-month-old control and RIPK1-tKO mice. Scale bars, 50 μm. (**L**) Quantitative polymerase chain reaction (qPCR) analysis for the expression of Ifng, Cxcl10, and Cd3e in sciatic nerve from 10-month-old control and RIPK1-tKO mice. (**M**) Survival of control ($n = 8$) and RIPK1-tKO ($n = 11$) mice. Error bars represent SEM. Data are representative of at least three independent experiments. *$P < 0.05$, **$P < 0.01$, ***$P < 0.005$, and ****$P < 0.001$ using Student's t test.

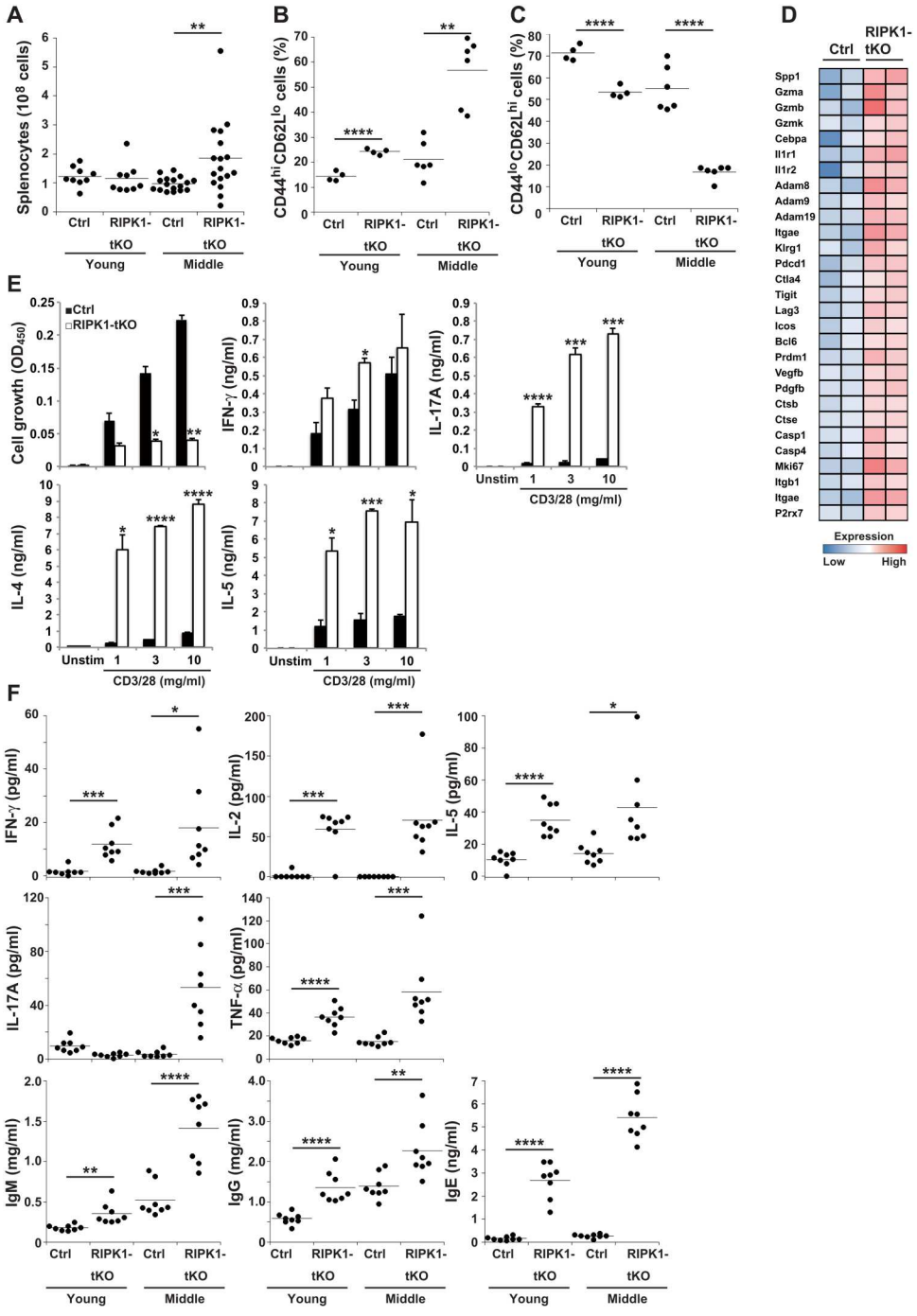

Fig. 2. RIPK1 deficiency in T cells induces CD4 T cell senescence. (**A**) Total cell numbers in the spleen of young ($n = 9$) and middle-aged ($n = 17$) control or RIPK1-tKO mice. (**B** and **C**) The percentage of $CD44^{hi}$ $CD62L^{lo}$ cells in CD4 T cells (B) and $CD44^{lo}$ $CD62L^{hi}$ cells in CD4 T cells (C) from the spleen of young ($n = 4$) and middle-aged ($n = 6$) control or RIPK1-tKO mice. (**D**) RNA-seq data showing the relative expression of senescence-related genes in $CD4^+$ $CD25^-$ T cells of spleen from 10-month-old control and RIPK1-tKO mice ($n = 2$). (**E**) $CD4^+$ T cells from control or RIPK1-tKO mice were stimulated with immobilized anti-CD3ε plus anti-CD28 (anti-CD3/CD28). Cell growth (top left) and cytokine production were assessed after 48 hours of stimulation by a water soluble tetrazolium salt-8 (WST-8) proliferation assay and electrochemiluminescence (ECL), respectively. OD_{450}, optical density at 450 nm; Unstim, unstimulated. (**F**) Serum cytokine levels in young and middle-aged control ($n = 8$) and RIPK1-tKO ($n = 8$) mice were determined by ECL. Error bars represent SEM. Data are representative of at least three independent experiments (E and F). $^*P < 0.05$, $^{**}P < 0.01$, $^{***}P < 0.005$, and $^{****}P < 0.001$ using Student's *t* test.

RIPK1-tKO mice develop age-associated diseases

Next, we examined whether RIPK1-KO T cells induce age-associated diseases. Because inflammaging is a risk factor for type 2 diabetes and recurrent hypoglycemia is common in elderly people (*27*), we first performed insulin tolerance tests (ITTs) and glucose tolerance tests (GTTs). Blood glucose levels were significantly decreased in RIPK1-tKO mice (Fig 3, A and B), although food intake and serum insulin levels were comparable to those of control mice (Fig. 3C and fig. S3A), suggesting that RIPK1-tKO mice develop hypoglycemia. Second, inflammaging plays a role in the increased risk of age-related sarcopenia, which is characterized by progressive loss of muscle mass, strength, and functions (*28*). The grip strength test revealed a reduction of skeletal muscle strength in RIPK1-tKO mice (Fig. 3D); consistently, tibialis muscle mass was markedly reduced (Fig. 3, E and F). Further, the increased expression of Ifng, Cxcl10, and Cd3e was observed in the tibialis muscle of RIPK1-tKO mice (Fig. 3G). These data indicate that RIPK1-KO T cells induced muscle inflammation and subsequent sarcopenia. Furthermore, RIPK1-tKO mice exhibited a marked reduction of adipose tissue mass and smaller adipocytes (fig. S3, B and C).

To evaluate the morbidity of RIPK1-tKO mice, serum metabolomic profiling was performed. (i) The serum kynurenine/tryptophan ratio as a biomarker of inflammaging and cancer (*29*, *30*) increased in both young and middle-aged RIPK1-tKO mice (Fig. 3H), confirming that RIPK1-KO T cells cause chronic inflammation from a young age. (ii) Because anemia of inflammation is prevalent in patients with inflammation, such as infections, autoimmune diseases, and cancer (*31*), the blood hemoglobin levels were assessed. We observed that middle-aged but not young RIPK1-tKO mice developed anemia (Fig. 3I). (iii) Serum-oxidized glutathione and ophthalmic acid, biomarkers of oxidative stress, which are thought to drive multiple age-related diseases (*32*–*35*), were increased in middle-aged but not young RIPK1-tKO mice (Fig 3H). Because the opacity of the lens is thought to be a direct result of oxidative stress (*36*), oxidative stress may cause the lens opacity observed in RIPK1-tKO mice (Fig. 1, C and D). Furthermore, (iv) serum symmetric and asymmetric dimethylarginine (SDMA and ADMA), known as risk factors for cardiovascular disease (*37*, *38*), increased in middle-aged but not young RIPK1-tKO mice (Fig. 3H). Inversely, serum carnitine, beneficial for cardiovascular diseases (*39*, *40*), was reduced in middle-aged but not young RIPK1-tKO mice (Fig. 3H). Consistently, RIPK1-tKO mice showed significant increases in heart /body weight ratios and increased expression of Ifng, Cxcl10, and Cd3e in the heart (Fig. 3, J and K), suggesting that RIPK1-KO T cells also induced cardiac inflammation. (v) We further observed that serum pantothenic acid (vitamin B5), which is significantly decreased in both Alzheimer′s disease and Huntington′s disease (*41*, *42*), was also decreased in middle-aged RIPK1-tKO mice (Fig. 3H). (vi) Serum uric acid, which is commonly elevated in subjects with chronic kidney disease (*43*, *44*), was increased in middle-aged RIPK1-tKO mice (Fig. 3I). Consistently, the activity of senescent-associated (SA) β-galactosidase was higher in kidneys from RIPK1-tKO mice than from control mice (Fig. 3M), indicating that senescence is also induced in the kidneys of RIPK1-tKO mice. Together, these data indicate that RIPK1 deficiency in T cells causes chronic inflammation and, consequently, the premature development of age-related multimorbidity.

RIPK1 inhibits the activation of Akt, mTORC1, and ERK signaling

To elucidate the molecular mechanism underlying the multiorgan cellular senescence induced by RIPK1-KO T cells, we sought to identify the signaling pathways regulated by RIPK1 by pathway analysis of genes up-regulated in RIPK1-KO CD4 T cells as compared to WT CD4 T cells. The expression of cell cycle–related genes was clearly up-regulated in RIPK1-KO CD4 T cells (Fig. 4A). Because the mTORC1 pathway is critical for cell cycle regulation upon TCR stimulation (*7*), the activation of mTORC1 signals in RIPK1-KO naïve CD4 T cells was assessed. RIPK1-KO naïve CD4 T cells ex vivo showed high basal levels of mTORC1 activation (phosphorylation of S6 and 4E-BP1) and ERK phosphorylation (fig. S4, A and B). We similarly observed that basal activation levels of mTORC1 and ERK, but not p38, were also enhanced in RIPK1-KO effector CD4 T [T helper (T_H)] cells and that this was impaired by treatment with rapamycin, an mTOR inhibitor (Fig. 4B and fig. S4C). RIPK1-KO T_H cells showed increased cell size, enhanced cell death, and decreased viable cells, which was also restored by rapamycin treatment (fig. S4, D to F). The basal activity of Akt, which is upstream of mTORC1 signals, was enhanced in RIPK1-KO T_H cells, whereas Phosphoinositide-dependent kinase 1(PDK1), upstream of Akt, was not activated in these cells (Fig. 4B). Next, we assessed whether the reduced activation of mTORC1 following rapamycin treatment affected the TCR-induced cytokine production and the expression of senescence-related genes in RIPK1-KO T_H cells. Increased expression of senescence-related genes and augmented production of IFN-g, IL-4, IL-5, and IL-6 in RIPK1-KO Th cells was remarkably inhibited by rapamycin-treatment (Fig. 4, C and D). Furthermore, the increased expression of senescence-related genes and the increase of mTORC1 activation in RIPK1-KO T_H cells were strongly abolished by blocking Akt activation with LY294002, an inhibitor of PI3K (fig. S4, G and H). These data suggest that RIPK1 controls mTOR signaling through regulating Akt activation.

Unlike RIPK1-KO T_H cells, RIPK1 kinase inactive ($RIPK1^{D138N/D138N}$) T_H cells showed normal basal activation of mTORC1 and cytokine production (Fig. 4E and fig. S4I), suggesting that the kinase activity of RIPK1 is dispensable for regulation of T cell senescence. Similar to RIPK1-KO T_H cells, aged WT T_H cells showed augmented basal activation of Akt, mTORC1 signals, and ERK; an increased cell size; and enhanced cytokine production, which were all reduced by rapamycin treatment (Fig. 4F and fig. S4, J to L).

Senescent cells have been shown to display metabolic changes such as increased glycolysis and mitochondrial oxidative phosphorylation (OXPHOS) (*45*). Glycolysis-induced metabolites modulate inflammatory responses by signal modulation, posttranscriptional and posttranslational modifications, and epigenetic remodeling (*46*). Because it has been shown that mTORC1 activation is required to regulate TCR-induced glycolysis and OXPHOS (*7*), we next analyzed the oxygen consumption rate (OCR), which assesses OXPHOS and extracellular acidification (ECAR), a measure of glycolysis. We found that RIPK1-KO T_H cells exhibited elevated levels of OXPHOS and glycolysis (Fig. 4, G and H, and fig. S4M) and that these increases were strongly inhibited by rapamycin treatment (Fig. 4, I and J, and fig. S4N). These data indicate that RIPK1 deficiency in T cells causes hyperactivation of mTOR, leading to metabolic alterations and, subsequently, inflammatory responses.

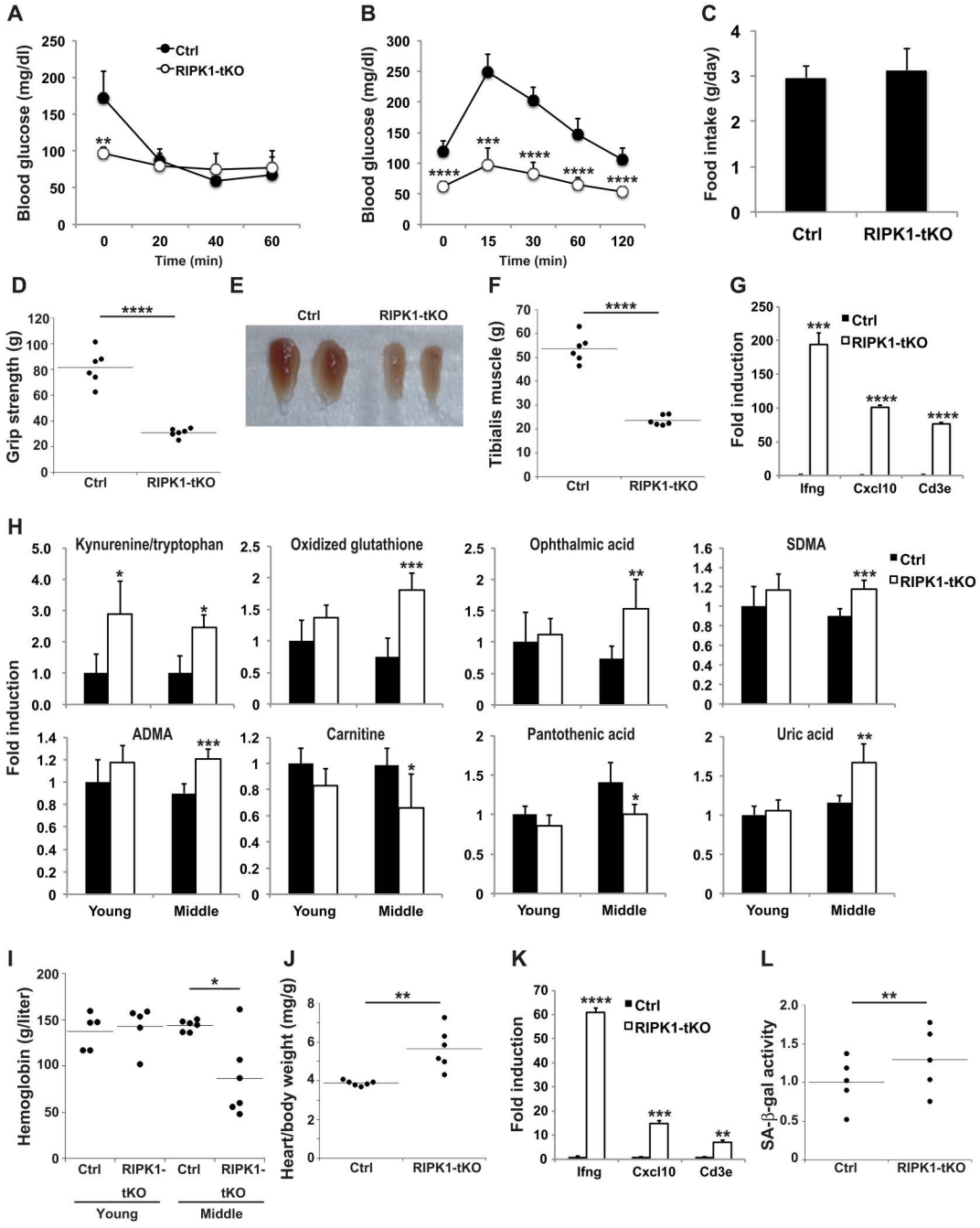

Fig. 3. RIPK1-tKO mice develop age-related diseases. (**A**) ITTs were performed in 6-month-old control ($n = 6$) and RIPK1-tKO ($n = 3$) mice. Mice were fasted for 4 hours and then injected intraperitoneally with insulin. Blood glucose levels were measured at the indicated times after insulin injection. (**B**) GTTs were performed in 6-month-old control ($n = 6$) and RIPK1-tKO ($n = 3$) mice. Mice were fasted for 16 hours, and glucose was then injected intraperitoneally. Blood glucose levels were measured at the indicated time points after glucose injection. (**C**) Food intake in 6-month-old control and RIPK1-tKO mice was measured for 24 hours. (**D**) Hindlimb grip strength analysis of 8-month-old control and RIPK1-tKO mice ($n = 6$ per group). (**E**) Representative photograph of the tibialis muscle from 7-month-old control and RIPK1-tKO mice. (**F**) Weight of tibialis muscle from 7-month-old control and RIPK1-tKO mice ($n = 6$ per group). (**G**) qPCR analysis for the expression of Ifng, Cxcl10, and Cd3e in the tibialis muscle from 12-month-old control and RIPK1-tKO mice. (**H**) Serum metabolome analysis of 10-month-old control and RIPK1-tKO mice. (SDMA and ADMA, respectively) ($n = 5$ per group). (**I**) Blood hemoglobin levels of young ($n = 5$) and middle-aged ($n = 6$) control and RIPK1-tKO mice were determined by enzyme-linked immunosorbent assay (ELISA). (**J**) Heart/body weight ratios of 10- to 13-month-old control and RIPK1-tKO mice ($n = 6$ per group). (**K**) qPCR analysis for the expression of Ifng, Cxcl10, and Cd3e in the heart from 12-month-old control and RIPK1-tKO mice. (**L**) Quantitative measurements of β-galactosidase (β-gal) activity in kidney lysates of 10- to 13-month-old control and RIPK1-tKO mice by colorimetric assay ($n = 5$ per group). Error bars represent SEM. Data are representative of at least three independent experiments (A to G and I to L). $^{*}P < 0.05$, $^{**}P < 0.01$, $^{***}P < 0.005$, and $^{****}P < 0.001$ using Student's t test.

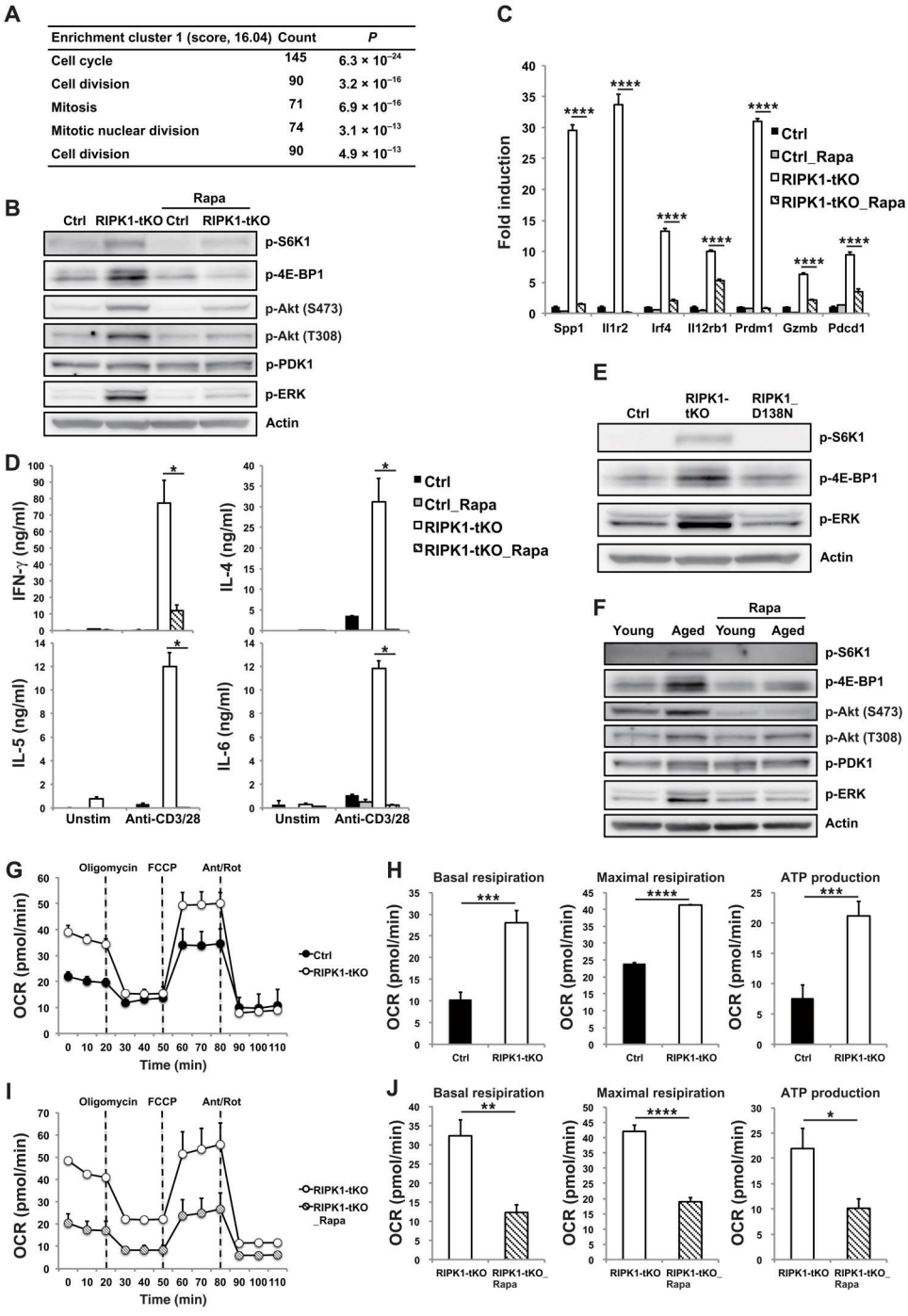

Fig. 4. Elevated activation of Akt, mTORC1, and ERK signaling in RIPK1-KO CD4 T cells. (**A**) Pathway enrichment analysis of gene expression with up-regulation in RIPK1-KO CD4 T cells as compared to WT CD4 T cells. Data were analyzed with DAVID Bioinformatics Resources 6.8. (**B**) $CD4^+$ $CD25^-$ $CD44^{lo}$ $CD62L^{hi}$ (naïve CD4) T cells from control or RIPK1-tKO mice were stimulated with anti-CD3/28 monoclonal antibody (mAb) in the presence or absence of rapamycin for 3 days, and cells were further cultured in the presence of IL-2 for 3 days. PI^- T_H cells were sorted and subjected to Western blot analysis of the indicated proteins (B) and qPCR analysis of the indicated genes (**C**) or stimulated with anti-CD3/28 mAb for 24 hours, and cytokine production was analyzed by ELISA (**D**). (**E** and **F**) Naïve CD4 T cells from control or RIPK1-tKO or $RIPK1^{D138N/D138N}$ mice (E) or young or aged mice (F) were stimulated with anti-CD3/28 mAb for 3 days, and then the cells were further cultured in the presence of IL-2 for 3 days. PI^- T_H cells were sorted and subjected to Western blot analysis of the indicated proteins. (**G**) Oxygen consumption rate (OCR) in T_H cells from control or RIPK1-tKO mice. (**H**) Basal respiration (left), maximal respiration (middle), and adenosine triphosphate (ATP) production (right) are shown. (**I**) OCR in T_H cells described in (B). (**J**) Basal respiration (left), maximal respiration (middle), and ATP production (right) are shown. Error bars represent SEM. Data are representative of at least three independent experiments (B to J). *$P < 0.05$, **$P < 0.01$, ***$P < 0.005$, and ****$P < 0.001$ using Student's t test.

Rapamycin treatment restores the function of RIPK1-KO T cells in vivo

Next, we investigated whether rapamycin treatment could also affect the senescent phenotype of RIPK1-KO T cells in vivo. Administration of rapamycin to RIPK1-tKO mice daily for 4 days decreased the percentage of $CD44^{hi}$ $CD62L^{lo}$ effector/memory phenotype CD4 T cells and increased the percentage of $CD44^{lo}$ $CD62L^{hi}$ naïve CD4 T cells (Fig. 5, A and B). The treatment also reduced the expression of senescence-related genes and the production of IFN-γ, IL-4, and IL-17A upon TCR stimulation by CD4 T cells and T_H cells from RIPK1-tKO mice compared to untreated RIPK1-tKO mice (Fig. 5, C and D, and fig. S5, A and B). Consistently, the serum levels of IFN-γ, IL-2, IL-5, TNF-α, and IgG were also decreased in these mice (Fig. 5E). These data indicate that enhanced activation of mTOR in RIPK1-KO T cells induces the senescence of T cells, which results in the elevated cytokine production in vivo and that this phenotype can be reversed by rapamycin treatment.

RIPK1 inhibits RIPK3- and caspase-8–mediated activation of Akt, mTORC1, and ERK signaling

A previous study demonstrating that RIPK1-KO T cells have elevated caspase activity (*24*) prompted us to determine whether

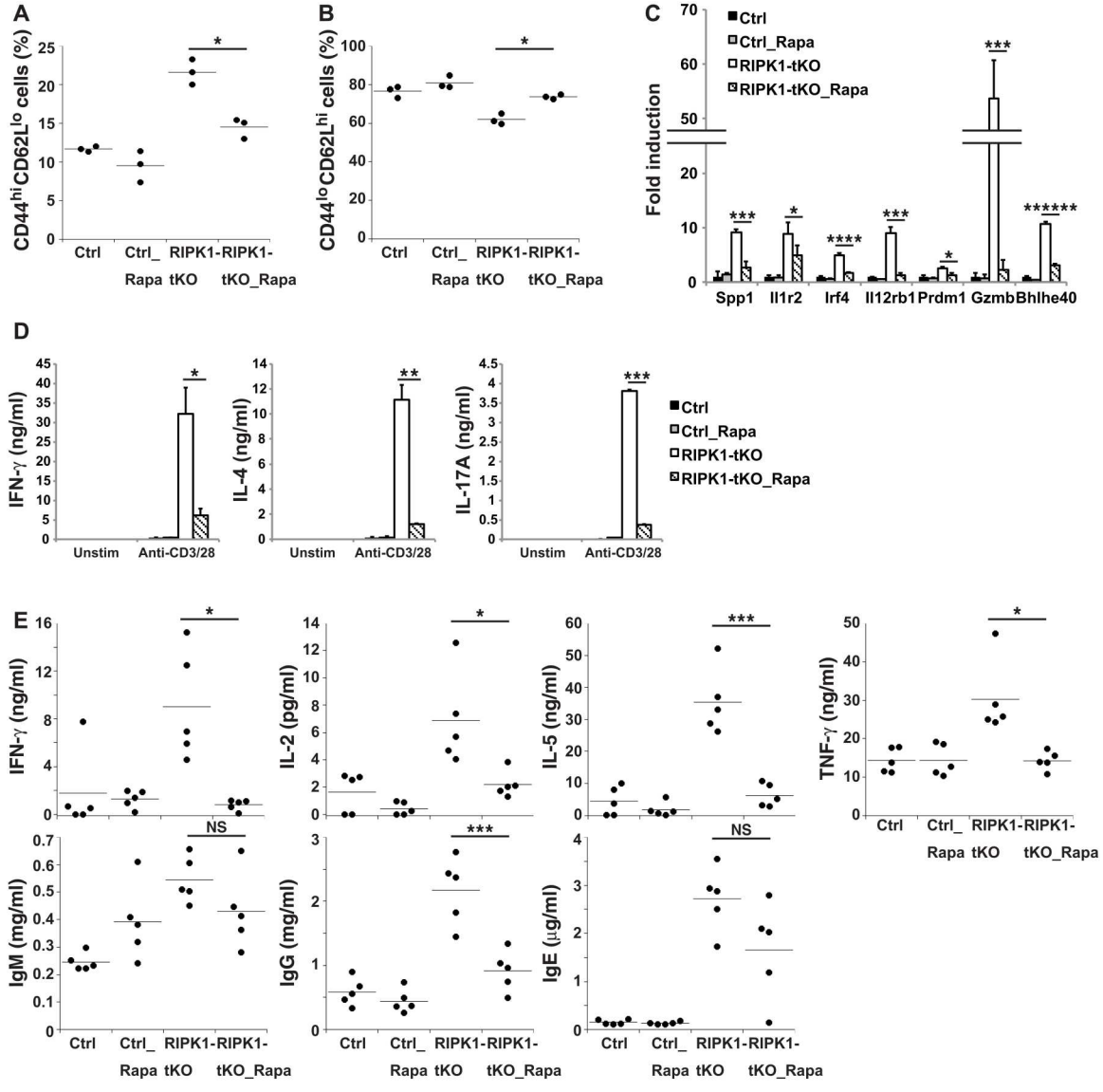

Fig. 5. Rapamycin inhibits CD4 T cell senescence in RIPK1-tKO mice. (**A**) The percentage of $CD44^{hi}$ $CD62L^{lo}$ cells (**B**) and $CD44^{lo}$ $CD62L^{hi}$ cells among CD4 T cells from spleen of control and RIPK1-tKO mice left untreated or treated daily with rapamycin for a total of 4 days ($n = 3$ per group). (**C**) qPCR analysis of the indicated genes in CD4 T cells from spleen of control and RIPK1-tKO mice left untreated or treated daily with rapamycin for a total of 4 days. (**D**) CD4 T cells from spleen of control and RIPK1-tKO mice left untreated or treated daily with rapamycin for a total of 4 days were stimulated with anti-CD3/28 mAb for 24 hours, and cytokine production was analyzed by ELISA. (**E**) Serum cytokine levels were determined by ECL in control and RIPK1-tKO mice left untreated or treated every other day with rapamycin for a total of 30 days ($n = 5$ per group). Error bars represent SEM. Data are representative of at least three independent experiments (A to E). *$P < 0.05$, **$P < 0.01$, ***$P < 0.005$, and ****$P < 0.001$ using Student's t test. NS, not significant.

increased basal activation of mTORC1 leads to augmentation of caspase activity. The levels of cleaved caspase-3, caspase-7, and poly(adenosine diphosphate–ribose) polymerase (PARP), which is the cleavage target of caspase-3, were increased in RIPK1-KO T_H cells (Fig. 6A). Treatment with rapamycin or LY294002 strongly reduced the levels of cleaved caspase-3, caspase-7, and PARP in RIPK1-KO T_H cells (Fig. 6A and fig. S6A). Similar results were obtained with aged WT T_H cells (Fig. 6B and fig. S6B), indicating that enhanced basal Akt-mTORC1 signaling induces the activation of caspase-3/7 in RIPK1-KO and aged CD4 T cells.

Because RIPK1 blocks caspase-8–dependent apoptosis and RIPK3-dependent necroptosis during development (*19*, *20*), it is likely that caspase-8 and RIPK3 are involved in the increased activation of Akt, mTORC1, and ERK signaling in RIPK1-KO T cells. To confirm this, we first used Z-IETD, an inhibitor specific for caspase-8. Treatment with Z-IETD results in partial reduction of the increased phosphorylation of Akt, mTORC1, and ERK and activation of caspase-3/7 in RIPK1-KO T_H cells (Fig. 6C). Z-IETD treatment also partially inhibited the expression of senescence-related genes in RIPK1-KO T_H cells except for Il1r2 (Fig. 6D). Similar results were obtained with caspase-8 knockdown RIPK1-KO T_H cells (Fig. 6E and fig. S6C), implying that RIPK1 inhibits the caspase-8–mediated activation of Akt, mTORC1, and ERK. We also analyzed whether the treatment with Z-IETD affects the

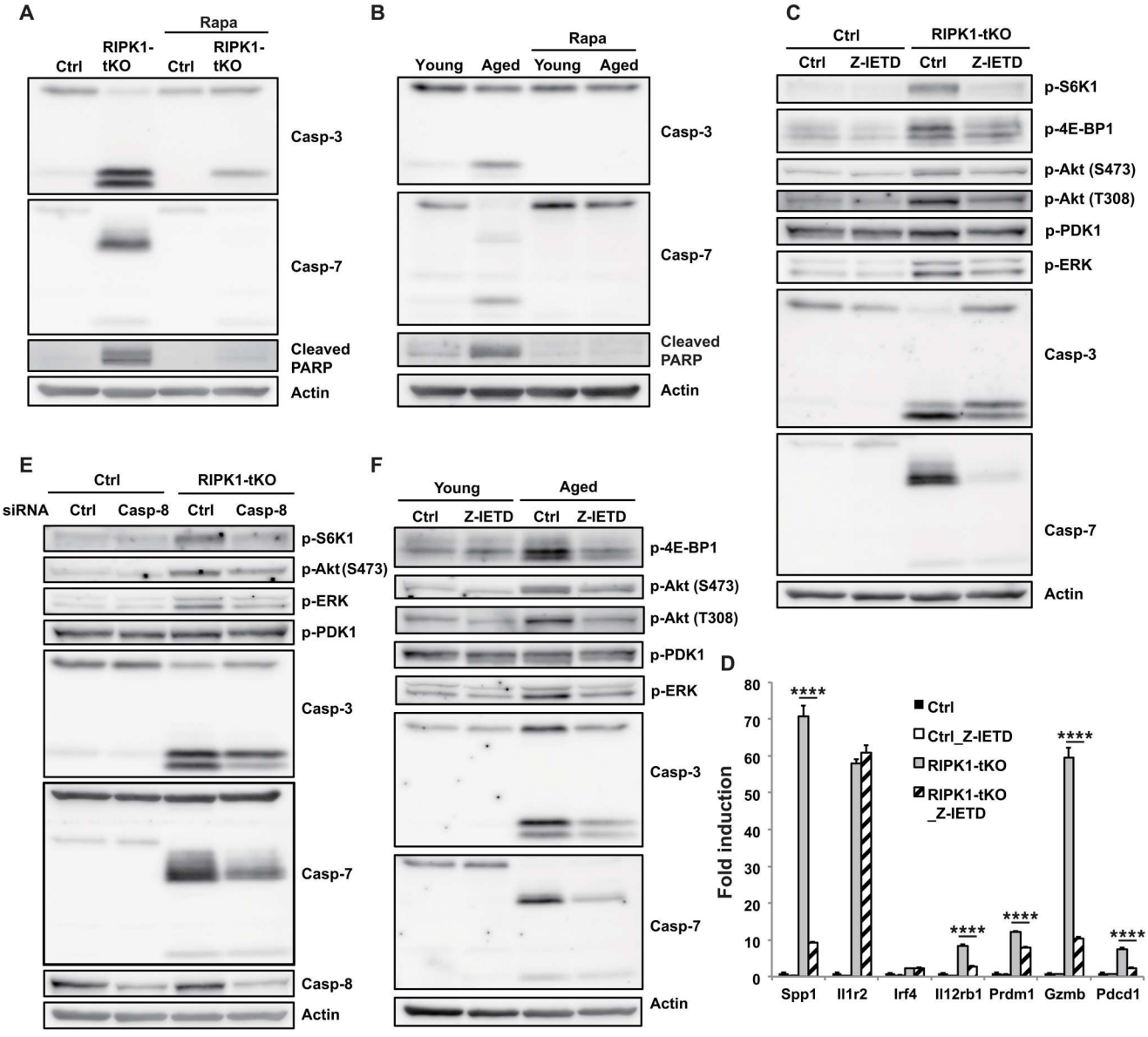

Fig. 6. RIPK1 inhibits the capsase-8 pathway. (**A** to **F**) Naïve CD4 T cells from control or RIPK1-tKO or young or aged WT mice were stimulated with anti-CD3/28 mAb for 3 days in the presence or absence of rapamycin or Z-IETD, and then the cells were further cultured in the presence of IL-2 for 3 days. PI^- T_H cells were sorted and subjected to Western blot analysis of the indicated proteins (A to C and F) or to qPCR analysis of the indicated genes (D). (E) CD4 T cells expressing small interfering RNA (siRNA) targeting caspase-8 (si-Casp-8) or control siRNA (si-Ctrl) were subjected to Western blot analysis. Error bars represent SEM. Data are representative of at least three independent experiments (A to F). ****$P < 0.001$ using Student's *t* test.

cell death level and the cell division of RIPK1-KO naïve CD4 T cells upon anti-CD3/28 stimulation. We found that the increased cell death but not the impaired cell division in RIPK1-KO CD4 T cells was partly restored by Z-IETD treatment (fig. S6, E and E). These data indicate that caspase-8 is critical for the increased cell death and the senescent phenotype caused by RIPK1 deficiency in T cells. Furthermore, Z-IETD treatment partially decreased the enhanced activation of mTORC1, Akt, ERK, and caspase-3/7 and the increased expression of senescence-related genes in aged T_H cells (Fig. 6F and fig. S6F). These data indicate that caspase-8 is involved in the induction of senescence in RIPK1-KO and normal CD4 T cells.

We then investigated the involvement of RIPK3 in this process by crossing RIPK1-tKO mice with RIPK3-KO mice (RIPK1/3-dKO mice). The decreased ratio and number of CD4 T cells in RIPK1-tKO mice were partially rescued by RIPK3 deficiency (Fig. 7, A and B). Further, the impaired proliferative response of RIPK1-KO naïve CD4 T cells upon anti-CD3/28 stimulation was partially restored by RIPK3 deficiency and almost fully restored in RIPK1/3-dKO T cells treated with Z-IETD or Z-VAD, a pan-caspase inhibitor (Fig. 7C). In addition, the enhanced activation of mTORC1, Akt, ERK, and caspase-3/7 was partially recovered in RIPK1/3-dKO T_H cells and almost fully recovered when these cells were treated with Z-IETD (Fig. 7D and fig. S7A). The enhanced production of IL-4 and IFN-γ and the decreased production of IL-2 were partly normalized in RIPK1/3-dKO T_H cells and more fully restored after treatment with Z-IETD (Fig. 7E and fig. S7B). Consistently, the increased expression of senescence-related genes in RIPK1-KO T_H cells was partly reduced by RIPK3 deficiency and almost fully rescued by RIPK3 deficiency and Z-IETD treatment (Fig. 7F and fig. S7C). The expression of RIPK3, but not RIPK1 and caspase-8, was up-regulated in $CD44^{hi}$ $CD62L^{lo}$ effector/memory phenotype CD4 T cells compared to $CD44^{lo}$ $CD62L^{hi}$ naïve CD4 T cells, suggesting the possible involvement of RIPK3 in the induction of T cell senescence. Together, these data suggest that both RIPK3 and caspase-8 are critical for the induction of T cell senescence by activating Akt, mTORC1, and ERK, which is blocked by RIPK1.

Environment affects the senescent phenotype of CD4 T cells

Because it has been shown that the SASP factors reinforce and propagate senescence (*5*), we next investigated whether the tissue environment of RIPK1-tKO mice converts the WT CD4 T cells into the senescent phenotype CD4 T cells by adoptive T cell transfer. We found that the percentage of $CD44^{hi}$ $CD62L^{lo}$ effector/memory phenotype CD4 T cells markedly increased (Fig. 8A), whereas that of $CD44^{lo}$ $CD62L^{hi}$ naïve CD4 T cells inversely decreased in WT T cells when transferred into RIPK1-tKO mice as compared to WT T cells before transfer (Fig. 8B). Consistently, the expression of senescence-related genes was up-regulated in WT T cells when transferred into RIPK1-tKO mice as compared to WT T cells before transfer (Fig. 8C). The cell numbers of WT CD4 T cells transferred into control or RIPK1-tKO mice were comparable (fig. S8A), suggesting that the phenotypic conversion of WT T cells into the senescent phenotype CD4 T cells in RIPK1-tKO mice is independent of homeostatic proliferation. Conversely, we next determined whether the normal tissue environment restores the RIPK1-KO CD4 T cells to the normal CD4 T cells. Consequently, the percentage of $CD44^{hi}$ $CD62L^{lo}$ effector/memory phenotype CD4 T cells markedly decreased (Fig. 8D), whereas that of $CD44^{lo}$ $CD62L^{hi}$ naïve CD4 T cells inversely increased in RIPK1-KO CD4 T cells transferred to WT mice (Fig. 8E). Consistently, the expression of senescence-related genes was down-regulated in RIPK1-KO T cells transferred into WT mice as compared to RIPK1-KO T cells before transfer (Fig. 8F). The cell number of RIPK1-KO CD4 T cells when transferred into a WT host was less than that of WT T cells transferred into a WT host (fig. S8B). These data indicate the possibility that T cell senescence caused by RIPK1 deficiency may not be a T cell–intrinsic effect, whereas the cell death caused by RIPK1 deficiency is a T cell–intrinsic effect.

To understand this mechanism more physiologically, we examined whether the normal tissue environment restores the aged CD4 T cells to the normal phenotype. The percentage of $CD44^{hi}$ $CD62L^{lo}$ effector/memory-type CD4 T cells markedly decreased (Fig. 8G), whereas that of $CD44^{lo}$ $CD62L^{hi}$ naïve CD4 T cells inversely increased in aged CD4 T cells transferred into young WT mice (Fig. 8H). Consistently, the expression of senescence-related genes was decreased in CD4 T cells transferred from aged mice into young WT mice as compared to aged CD4 T cells before transfer (fig. S8C). The cell numbers of young and aged CD4 T cells transferred into young WT mice were comparable (fig. S8D). These data suggest that the senescent phenotype of aged CD4 T cells is restored in the normal tissue environment.

We further determined whether the coculture environment of WT and RIPK1-KO T_H cells affects the phenotype of each T_H cells in vitro. The expression levels of senescence-related genes were strongly inhibited in RIPK1-KO T_H cells when cocultured with WT T_H cells as compared to RIPK1-KO T_H cells alone. On the other hand, those of senescence-related genes were not altered in WT T_H cells when cocultured with RIPK-KO T_H cells compared to WT T_H cells alone (Fig. 8I). Consistent with these results, the elevated activation of Akt, mTORC1, ERK, and caspase-3/7 was inhibited in RIPK1-KO T_H cells when cocultured with WT T_H cells as compared to RIPK1-KO T_H cells alone (Fig. 8J). Furthermore, the aberrant production of IL-2, IL-4, and IFN-γ was restored in RIPK1-KO T_H cells when cocultured with WT T_H cells (fig. S8E). It is noted that the cell number of RIPK1-KO T_H cells cocultured with WT T_H cells was much less than of WT T_H cells cocultured with RIPK1-KO T_H cells, and it was comparable to RIPK1-KO T_H cells cultured alone (fig. S8F). Therefore, the relative cell numbers of CD4 T cells originated from WT or RIPK1-KO CD4 T cells may determine the tissue and culture environment, which influence inducing senescence. These data indicate that the environment cocultured with WT T_H cells restores the senescent phenotype and the enhanced activation of Akt, mTORC1, ERK, and caspase-3/7 without altering the increased cell death in RIPK1-KO T_H cells. Collectively, these data indicate that the environmental signals are critical to determine the senescent phenotype of CD4 T cells by modulating mTOR signaling.

DISCUSSION

Biallelic mutations in *RIPK1* cause combined immunodeficiency and inflammatory diseases in humans. Our studies show that RIPK1 deficiency in T cells is sufficient for the development of inflammatory diseases in mice, ultimately leading to premature death. Similar to RIPK1-tKO mice, human RIPK1 deficiency causes lymphopenia and splenomegaly (*22*, *23*), suggesting that RIPK1 in T

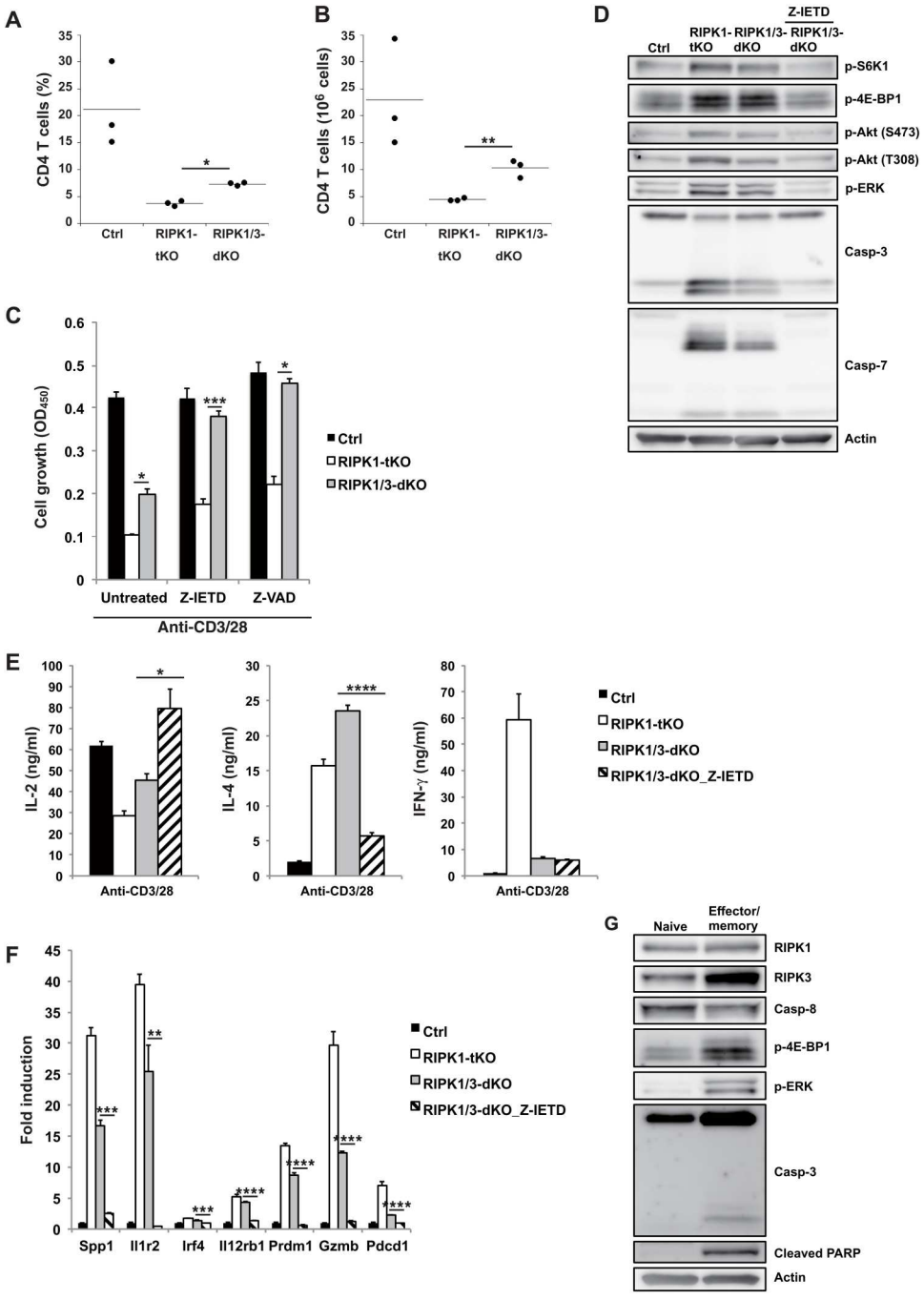

Fig. 7. RIPK1 inhibits the RIPK3- and caspase-8–mediated activation of Akt, mTORC1, and ERK pathways. (**A**) The percentage and number (**B**) of CD4 T cells from spleen of control, RIPK1-tKO, and RIPK1/3-dKO mice. (**C**) Naïve $CD4^+$ T cells from control or RIPK1-tKO or RIPK1/3-dKO mice were stimulated with anti-CD3/CD28 in the presence or absence of Z-IETD or Z-VAD. Cell growth was assessed after 48 hours of stimulation by a WST-8 proliferation assay. (**D** to **F**) Naïve CD4 T cells from control or RIPK1-tKO or RIPK1/3-dKO mice were stimulated with anti-CD3/28 mAb for 3 days in the presence or absence of Z-IETD, and then the cells were further cultured in the presence of IL-2 for 3 days. PI^- T_H cells were sorted and subjected to Western blot analysis of the indicated proteins (D) or qPCR analysis (F) or stimulated with anti-CD3/28 mAb for 24 hours, and cytokine production was analyzed by ELISA (E). (**G**) $CD44^{lo}$ $CD62L^{hi}$ naïve CD4 T cells and $CD44^{hi}$ $CD62L^{lo}$ effector/memory phenotype CD4 T cells were sorted and subjected to Western blot analysis of the indicated proteins. Error bars represent SEM. Data are representative of at least three independent experiments (A to H). *$P < 0.05$, **$P < 0.01$, ***$P < 0.005$, and ****$P < 0.001$ using Student's *t* test.

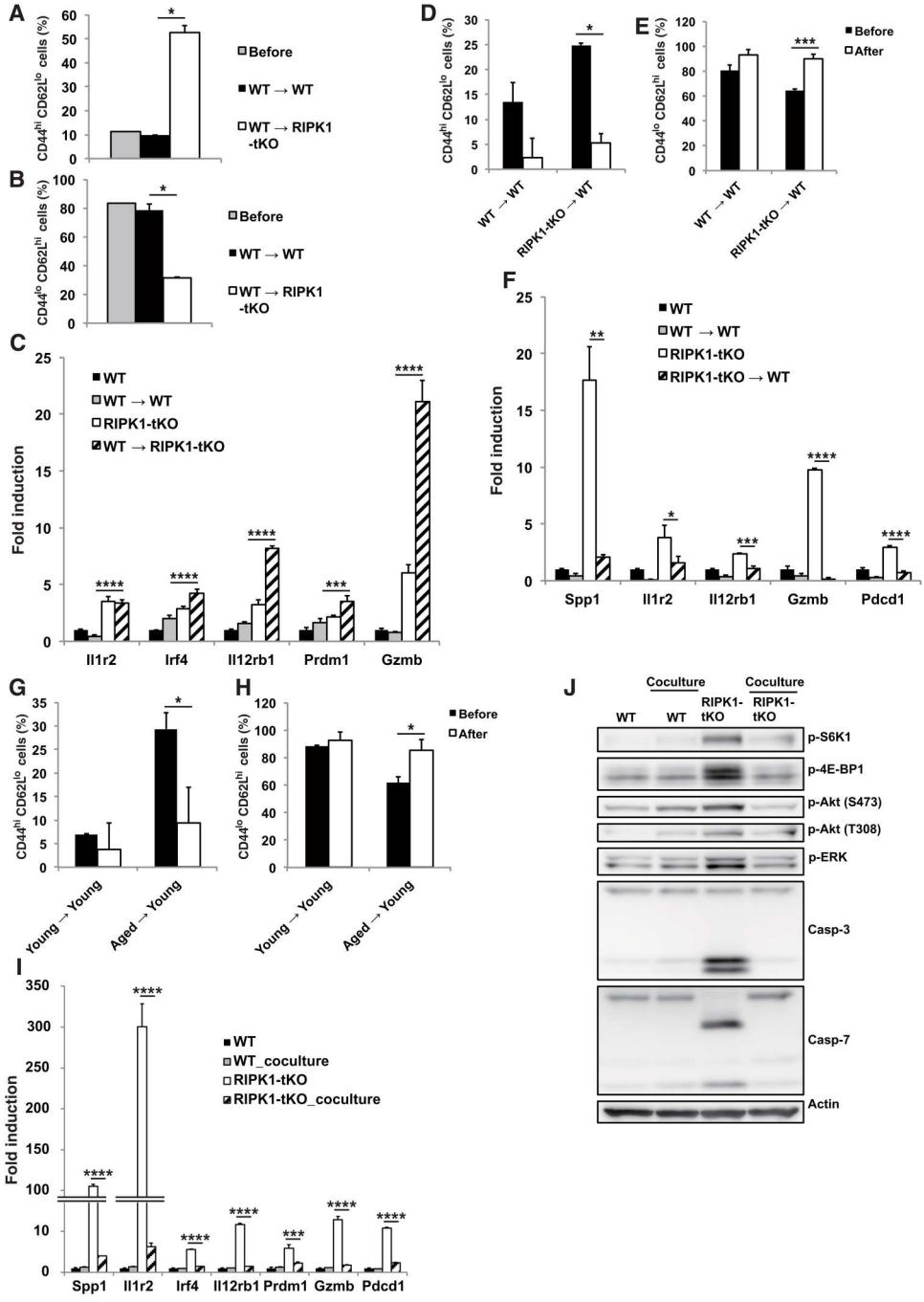

Fig. 8. Environment affects the senescent phenotype of CD4 T cells. (**A** to **C**) WT (CD45.1$^+$) CD4$^+$ CD25$^-$ T cells were transferred into WT or RIPK1-tKO mice, and the percentage of CD44^{hi} CD62L^{lo} cells (A) and CD44^{lo} CD62L^{hi} cells (B) among CD45.1$^+$ CD4 T cells of WT and RIPK1-tKO mice (n = 2 per group) was determined by flow cytometry. CD45.1$^-$ CD4 T cells from WT and RIPK1-tKO recipients and CD45.1$^+$ CD4 T cells from WT (WT → WT) and RIPK1-tKO (WT → RIPK1-tKO) mice were collected and subjected to qPCR analysis (C). (**D** to **F**) CD4$^+$ CD25$^-$ T cells from WT and RIPK1-tKO mice were transferred into WT (CD45.1$^+$) mice, and the percentage of CD44^{lo} CD62L^{hi} cells (D) and CD44^{hi} CD62L^{lo} cells (E) among CD4 T cells from WT and RIPK1-tKO mice (n = 2 per group) was determined by flow cytometry. WT and RIPK1-KO CD4 T cells before transfer and WT (WT → WT) and RIPK1-KO (RIPK1-tKO → WT) CD4 T cells from CD45.1$^+$ mice were collected and subjected to qPCR analysis (F). (**G** and **H**) CD4$^+$ CD25$^-$ T cells from young and aged mice were transferred into young WT (CD45.1$^+$) mice, and the percentage of CD44^{lo} CD62L^{hi} cells (G) and CD44^{hi} CD62L^{lo} cells (H) among CD4 T cells from young and aged mice (n = 2 per group) was determined by flow cytometry. (**I** and **J**) Naïve CD4 T cells from WT (CD45.1$^+$) or RIPK1-tKO mice were cocultured at a ratio of 1 to 1, or cultured alone, upon anti-CD3/28 mAb stimulation for 6 days. PI$^-$ T_H cells were sorted and subjected to qPCR analysis (I) and Western blot analysis (J). Error bars represent SEM. Data are representative of at least two independent experiments (A to J). *P < 0.05, **P < 0.01, ***P < 0.005, and ****P < 0.001 using Student's t test.

cells may play a critical role in controlling human inflammatory diseases.

We further demonstrated that RIPK1 deficiency in T cells results in T cell senescence, which is sufficient to cause age-associated features including chronic tissue inflammation, neurodegeneration, sarcopenia, anemia, and hypoglycemia, indicating the critical role of T cells in these age-related pathologies.

Mechanistically, RIPK1-KO CD4 T cells exhibit elevated basal activation of Akt, mTORC1, and ERK, leading to the enhanced expression of senescence-related genes and production of proinflammatory cytokines. Such basal activation of these genes is restored by a combined deficiency of RIPK3 and caspase-8 inhibition, indicating that activation of RIP3K/caspase-8 leads to senescence. Aged WT T cells exhibit enhanced basal activation of Akt, mTORC1, and ERK signaling similar to RIPK-KO T cells, and the treatment with rapamycin or a caspase-8 inhibitor corrects the dysfunction of these aged T cells. Our findings indicate that the RIPK3 and caspase-8 pathways are involved in basal signal activation in aged T cells under physiological conditions, suggesting that RIPK1 and RIPK3/caspase-8 may be potentially important therapeutic targets for delaying aging and age-associated diseases.

We showed that host environment affects the senescent phenotype of transferred CD4 T cells. The senescent phenotype of aged and RIPK1-KO CD4 T cell is restored in the normal tissue environment. Coculture experiments consistently revealed that relatively large numbers of young CD4 T cells induce the restoration of the enhanced expression of senescence-related genes and the increased activation of mTOR in RIPK1-KO CD4 T cells. These data suggest the possibility that the enhanced activation of mTOR in aged and RIPK1-KO CD4 T cells may not merely be T cell–intrinsic effects but rather modulated by the environmental signals. Therefore, environmental signals are likely to be critical for the modulation of T cell senescence. mTOR activations are tuned by such multiple environmental signals as TCR, costimulatory molecules, cytokines, growth factors, nutrients, oxygen, and metabolites (*6*). Therefore, there might be two possible mechanisms: T cell–intrinsic and environmental signals for the induction of senescent CD4 T cells by RIPK1 deficiency. One is that enhanced activation of mTOR, which was caused by RIPK1 deficiency and mediated by RIPK3/caspase-8, initiates the conversion into the senescent T cells. This conversion is induced in a T cell–intrinsic manner and amplified by the environmental signals in RIPK1-tKO mice. Another possibility is that the environment where massive T cell death is induced by RIPK1 deficiency promotes the activation of mTOR, leading to T cell senescence. Further investigation is required to elucidate the mechanism by which the normal environmental signals restore the senescent phenotype of aged and RIPK1-KO CD4 T cells.

Recent studies reported that a metabolic disorder in mitochondrial regulation in T cells induced T cell senescence and age-associated inflammation (*47*–*49*). Our studies revealed that RIPK1 is a key molecule for T cell metabolism by modulating mTOR signaling. A recent study reported that RIPK1 is involved in regulating TSC2 (an upstream negative regulator of mTORC1) phosphorylation by AMPK, which resulted in elevated mTORC1 activity in mouse embryonic fibroblasts (MEFs) and a human colon cancer cell line (*50*). Furthermore, another report demonstrated that RIPK1 deficiency increases aspartate levels, which enhances the tricarboxylic acid (TCA) flux and adenosine triphosphate (ATP) production, leading to defective autophagy induction by inhibiting the AMP-activated protein kinase (AMPK)/unc-51 like autophagy activating kinase 1 (ULK1) pathway in MEFs (*51*). In this case, RIPK1 regulates aspartate metabolism by inhibiting specificity protein 1 (SP1) nuclear expression, probably by altered phosphorylation (*51*). However, our RNA-seq data showing that expression of genes related to aspartate catabolism was not down-regulated in RIPK1-KO CD4 T cells indicate that regulation of mTOR signaling by RIPK1 may be cell context dependent.

We have clarified the mechanism of RIPK1 to regulate the activation of Akt/mTORC1/ERK in RIPK1-tKO mice and its similarity to aged T cells. However, how basal activation of Akt/mTORC1/ERK in normal aged T cells is increased as in RIPK1-KO T cells is still unclear. Because a caspase-8 inhibitor partly inhibits the activation of Akt, mTORC1, ERK, and caspase-3/7, as well as the expression of senescence-related genes in aged CD4 T cells, caspase-8 is involved in the induction of T cell senescence in a physiological setting. In addition, considering that the expression level of RIPK3 but not RIPK1 is increased in aged effector/memory phenotype CD4 T cells, it is possible that activation of RIPK3 and caspase-8 may be enhanced, although the inhibitory function of RIPK1 remains unchanged with aging. A recent study showed that the down-regulation of deoxyribonuclease 2 (DNase2) and Three prime repair exonuclease 1 (TREX1) expression causes the cytoplasmic accumulation of DNA in senescent cells, leading to the SASP by the aberrant activation of cyclic GMP-AMP synthase (cGAS)-Stimulator of interferon genes (STING) pathway (*52*). In the similar line, another study has shown that DNA is accumulated in the cytoplasm of aged CD4 T cells (*53*). However, in this case, the cytoplasmic DNA is sensed by the KU complex but not STING and activates leucine zipper and sterile α motif kinase (ZAK), which then activates Akt and mTORC1 pathways (*53*). Therefore, it is possible that the activation of RIPK3 and caspase-8 may be enhanced upon DNA sensing by the KU complex with aging in T cells. Accordingly, RIPK3 and caspase-8 might be involved in the regulation of ZAK activation in aged T cells.

Because RIPK1 interacts with caspase-8 through the FAS-associated death domain protein (FADD) adaptor protein in TNF-α signaling, it is likely that RIPK1 inhibits caspase-8–mediated activation of Akt, mTORC1, and ERK through FADD in T cells. Although previous studies reported that caspase-8 is essential for T cell activation in addition to its critical roles in apoptosis in both humans and mice (*54*, *55*), the molecular mechanisms underlying caspase-8–mediated T cell activation remain unsettled despite extensive studies. On the basis of our analyses, caspase-8 may be involved in the basal activation of Akt, mTORC1, and ERK pathways in T cells and that RIPK1 regulates caspase-8 function.

Increasing evidence suggests that mTORC1 is a critical regulator for aging. Long-term rapamycin treatment or genetic inhibition of mTORC1 signaling could extend the life span of mice (*56*, *57*). Furthermore, mTOR inhibition improved the response to the influenza vaccine and reduced the percentage of CD4 and CD8 T cells expressing Programmed cell death 1 (PD-1), which increases with age, in elderly humans (*58*). It will be an intriguing study to determine whether inhibition of mTORC1 signaling specifically in T cells can extend life span.

We found that increased activation of mTORC1 results in the activation of caspase-3/7 in RIPK1-KO and aged T cells. Consistent with our results, TSC1-KO T cells exhibit higher caspase activity (*8*). Mechanistically, loss of TSC1 or TSC2 causes endoplasmic

reticulum stress and activates the unfolded protein response, which leads to apoptosis in MEFs (*59*). Although the physiological role of noncanonical caspase-3/7 activation mediated by hyperactivation of mTORC1 in T cells remains unclear, caspase-3/7 activation could be a useful senescence marker for T cells.

Together, our results demonstrate that RIPK1 deficiency triggers the activation of RIPK3/caspase-8 and then mTORC1, which is critically involved in inducing T cell senescence, and that senescence-inducing signals are modulated by the environmental signals. The observation that RIPK1 deficiency in T cells causes age-related diseases and premature death in mice provides impetus for further clinical studies and the development of new therapeutic strategies targeting RIPK1 and RIPK3/caspase-8 for age-related diseases.

METHODS

Animals

C57BL/6J mice were purchased from Clea Japan Inc. *Ripk1*$^{fl/fl}$ and *Ripk1*$^{D138N/D138N}$ mice were provided by M.P. (University of Cologne). *Ripk3*$^{-/-}$ mice were provided by Genentech Inc. Foxp3YFP-Cre and CD45.1 mice were purchased from The Jackson Laboratory. Male and female mice of 2 to 26 months old were used. Two to 4, 6 to 10, and 20 to 26 months old were used as young, middle-aged, and aged mice, respectively. All mice were maintained under specific pathogen–free conditions at RIKEN, and all experiments were conducted under protocols approved by the RIKEN Yokohama Institute.

Reagents and antibodies

Rapamycin, Z-IETD-FMK, Z-VAD-FMK, and LY294002 were obtained from Merck. Antibodies (Abs) specific for anti-phospho-S6K1 (#9205; 1:500 dilution), anti–phospho-S6 (#2211; 1:10,000 dilution), anti–phopho-4E-BP1 (#9459; 1:1000 dilution), anti–phospho-Akt (S473) (#9271; 1:1000 dilution), anti–phospho-Akt (T308) (#4056; 1:500 dilution), anti–phospho-ERK1/2 (#9101; 1:1000 dilution), anti-cleaved PARP (#9548; 1:1000 dilution), anti–caspase-3 (#9662; 1:1000 dilution), anti–caspase-7 (#9492; 1:1000 dilution), anti–phospho-PDK1 (Ser^{241}) (#3061; 1:1000 dilution), anti–phospho-p38 (#9211; 1:1000 dilution), anti–β-actin (#4967; 1:10,000 dilution), anti–phospho-S6-PE (#5316; 1:50 dilution), and anti–phospho-4E-BP1-PE (#7547; 1:50 dilution) were obtained from Cell Signaling Technology; anti–caspase-8 (ALX-804-447; 1:1000 dilution) was obtained from Enzo. Flow cytometric analysis was performed on LSRFortessa X-20, and data were analyzed with FlowJo.

Cell preparation

CD4$^+$ naïve T cells were purified from spleen and lymph nodes as CD4$^+$/CD25$^-$/NK1.1$^-$/CD44^{low}/CD62L^{high} cells by sorting using a FACSAria (BD Biosciences). T_H cells were prepared by stimulation of naïve CD4$^+$ T cells with plate-bound anti-CD3ε (2C11; 10 μg/ml) and anti-CD28 (PV-1; 10 μg/ml) (anti-CD3/CD28) in the presence or absence of rapamycin (100 nM) or LY294002 (10μM) or Z-IETD (50 μM) for 3 days, and then the cells were washed and further cultured in the presence of IL-2 (10 ng/ml) for 3 days in RPMI 1640 supplemented with 10% fetal calf serum, and then Propidium iodide (PI)$^-$ live cells were sorted using a FACSAria.

Functional analyses

Naïve CD4 T cells and T_H cells were stimulated with immobilized anti-CD3ε (10 μg/ml) and anti-CD28 (5 μg/ml). Culture supernatants were analyzed by enzyme-linked immunosorbent assay (ELISA) for production of IL-2, IL-4, and IFN-γ (BD Biosciences) or electrochemiluminescence (ECL) using the V-PLEX Proinflammatory Panel 1 Mouse Kit (K15048D, Meso Scale Diagnostics). Sera were analyzed by ECL using the V-PLEX Proinflammatory Panel 1 Mouse Kit or U-PLEX mouse IL-17A assay (K152UTK; Meso Scale Diagnostics) or ELISA using mouse IgM, IgG, and IgE ELISA kits (Bethyl Laboratories); mouse anti-dsDNA ELISA kit (AKRDD-061, FUJIFILM); and mouse insulin ELISA kit (Mercodia Uppsala, Sweden). Cell growth was assessed using a cell counting kit-8 (Dojindo).

Real-time quantitative polymerase chain reaction

After removal of genomic DNA by treatment with DNase (Wako Nippon Gene), randomly primed cDNA strands were generated with reverse transcriptase III (Invitrogen). RNA expression was quantified by real-time polymerase chain reaction (PCR) with gene-specific primers, and values were normalized to the expression of *Rps18* mRNA. Quantitative PCR (qPCR) was performed with the Fast Syber Green Master Mix (Applied Biosystems). Data were collected and calculated by using the StepOnePlus real-time PCR system (Applied Biosystems).

Western blot analysis

Cells were lysed in 1% NP-40 lysis buffer [1% NP-40, 50 mM tris, 150 mM NaCl, 5 mM EDTA, aprotinin (10 μg/ml), chymostatin (12.5 μg/ml), leupeptin (50 μg/ml), pepstatin A (25 μg/ml), 1 mM phenylmethylsulfonyl fluoride, and 2 mM Na_3VO_4]. The lysates or immunoprecipitates were subjected to SDS–polyacrylamide gel electrophoresis and then transferred to membranes. Western blots were conducted by reacting the membrane with specific Ab and developed with an enhanced chemiluminescence assay according to the manufacturer's recommendations (Pierce).

RNA interference

Double-stranded oligonucleotides corresponding to the target sequences were cloned into the pSuper.Retro RNAi plasmid (OligoEngine Inc.). The small interfering RNA (siRNA) targeting sequence of caspase-8 is 5′-GGAAGATCGAGGATTATGAAA-3′. Constructs were transiently transduced into Phoenix packaging cells (provided by G. Nolan, Stanford University) using Lipofectamine with PLUS reagent (Invitrogen). Naïve CD4 T cells were stimulated with plate-bound anti-CD3/CD28 monoclonal Abs (mAbs), and cells were transduced by centrifugation at 1640*g* for 90 min in retroviral supernatants and polybrene (8 μg/ml) (Sigma-Aldrich) on day 1 after stimulation. After 72 hours of stimulation, green fluorescent protein–positive cells were sorted with FACSAria.

RNA-seq analysis

Total RNA was isolated from T cells using the Direct-zol RNA kit (Zymo Research) according to the manufacturer's instructions. The DNA library for RNA-seq analysis was constructed with a NEBNext Ultra RNA Library Prep Kit for Illumina (New England Biolabs Inc., Ipswich, MA) according to the manufacturer's instruction. The size range of the resulting DNA library was estimated on a 2100

Bioanalyzer (Agilent Technologies). The DNA library was subjected to the HiSeq 1500 sequencing system (Illumina) in a single-end read mode to obtain the sequencing data. The sequence reads were mapped to the *Mus musculus* reference genome [National Center for Biotechnology Information (NCBI) version 37] using TopHat2 version 2.0.8 and botwie2 version 2.1.0 with default parameters, and gene annotation was provided by NCBI. According to the mapped data, Cufflinks (version 2.1.1) was used to calculate the FPKM (fragments per kilobase per million mapped reads) values. Pathway enrichment analysis was done using DAVID Bioinformatics Resources 6.8 (*60*). Heatmaps were produced from normalized expression data referring to DAVID Bioinformatics Resources 6.8.

Clinical scoring

Limb grip strength was measured using a grip strength test apparatus (Bioseb). For the hindlimb reflex score, mice were suspended from their tails, and the hindlimb reflex score was evaluated using an established definition: 0, normal; 1, failure to stretch their hindlimbs; 2, hindlimb clasping; and 3, hindlimb paralysis. The severity of eye opacity was scored using the following definition: 0, normal; 1, one teary eye; 2, both teary eyes; 3, one cloudy eye; 4, one teary eye and one cloudy eye; and 5, both cloudy eyes.

ITTs and GTTs

After fasting for 4 hours, 15 μl of Humulin R (100 U/ml) (Eli Lilly and Company, Indianapolis, IN) was diluted in 7.2 ml of saline and administrated intraperitoneally at 3.6 μl/g of body weight (0.75 mU/g of body weight). Blood glucose levels were measured immediately before administration (0 min) and at 20, 40, and 60 min using an ACCU-CHEK ST Meter (Roche) from the tail vein.

A glucose solution (20%) was prepared by diluting 50% glucose (Otsuka Pharmaceutical Factory, Naruto, Japan) with distilled water. After fasting for 16 hours, the 20% glucose solution was intraperitoneally administrated at 10 μl/g of body weight (2 mg/g of body weight), and blood glucose levels were determined using an ACCU-CHEK ST Meter (Roche) immediately before administration (0 min) and at 15, 30, 60, and 120 min from the tail vein.

Metabolic assays

The OCR and ECAR in T_H cells were measured in an XFp extracellular flux analyzer (Seahorse Bioscience) using the XFp Cell Mito Stress Test Kit. The parameters used in the assays were the following: 2.5×10^4 cells per well, 1 μM oligomycin, 2 μM carbonyl cyanide *p*-trifluoromethoxyphenylhydrazone, 0.5 μM rotenone/antimycin A, 10 mM glucose, and 50 mM 2-deoxyglucose, as indicated.

Liquid chromatography–tandem mass spectrometry analysis

The liquid chromatography–tandem mass spectrometry analysis of metabolites in serum from 10-month-old control or RIPK1-tKO mice was performed using a Nexera X2 system (Shimadzu Corp.) equipped with two LC-30 AD pumps, a DGU-$20A_{5R}$ degasser, an SIL-30 AC autosampler, a CTO-20 AC column oven, and a CBM-20A control module, coupled with an LCMS-8060 triple quadrupole mass spectrometer (Shimadzu Corp.). A pentafluorophenylpropyl column (Discovery HS F5; 150 mm by 2.1 mm, 3 μm; Sigma-Aldrich) was used for the separation of metabolites. The mobile phase was composed of A, 0.1% (v/v) formic acid in water, and B, 0.1% (v/v) formic acid in acetonitrile. The flow rate, column temperature, and injection volume were set as 0.25 ml/min, 40°C, and 3 μl, respectively. The gradient program for mobile phase B was as follows: 0 min, 0%; 2 min, 0%; 5 min, 25%; 11 min, 35%; 15 min, 95%; 20 min, 95%; 20.1 min, 0%; and 25 min, 0%. The mass spectrometer was equipped with an electrospray ionization source.

Histological analysis

Lungs, salivary glands, tibialis muscles, and visceral adipose tissue were fixed for at least 24 hours with 4% paraformaldehyde and then embedded in paraffin. Sections were stained with hematoxylin (Sakura Fintek Japan) and eosin (Sakura Fintek Japan) and examined by light microscopy (BZ-X810, KEYENCE).

Sciatic nerves were removed, cut, and fixed with 2% glutaraldehyde and 2% paraformaldehyde in 0.1 M phosphate buffer (pH 7.4). Samples were washed twice in phosphate buffer and postfixed in osmium tetroxide, then dehydrated in an ascending ethanol gradient, and then embedded in epoxy resin. Semithin sections (0.5 μm) were cut using an ultramicrotome and stained with 1% toluidine blue sodium borate stain.

SA β-galactosidase assay

For the β-galactosidase quantitative assay, kidney was lysed with the T-PER Tissue Protein. Extraction reagent (Thermo Fisher Scientific, 78510) was used, lysates were centrifuged, and the supernatant was collected. Lysates were mixed with 50 μl of Pierce β-galactosidase assay reagent (Thermo Fisher Scientific, 75705) and incubated for 30 min, and then the absorbance was measured at 405 nm.

Adoptive transfer experiment

A total of 3×10^6 CD45.1 WT $CD4^+$ $CD25^-$ T cells were transferred into WT or RIPK1-tKO mice, and transferred cells were collected 7 days after transfer and subjected to flow cytometric and qPCR analysis. A total of 3×10^6 WT or RIPK1-KO or aged $CD4^+$ $CD25^-$ T cells were transferred into CD45.1 WT mice, and transferred cells were collected 4 days after transfer and subjected to flow cytometric and qPCR analysis.

Quantification and statistical analysis

Statistical significance was determined by a two-tailed unpaired Student's *t* test using KaleidaGraph (Synergy Software). Data are presented as the mean ± SEM values. $P < 0.05$ was considered statistically significant.

Supplementary Materials

This PDF file includes:

Figs. S1 to S8

View/request a protocol for this paper from *Bio-protocol*.

REFERENCES AND NOTES

1. C. Franceschi, J. Campisi, Chronic inflammation (inflammaging) and its potential contribution to age-associated diseases. *J. Gerontol. A Biol. Sci. Med. Sci.* **69**, S4–S9 (2014).
2. C. Franceschi, P. Garagnani, G. Vitale, M. Capri, S. Salvioli, Inflammaging and 'Garb-aging'. *Trends Endocrinol. Metab.* **28**, 199–212 (2017).

3. A. C. Maue, E. J. Yager, S. L. Swain, D. L. Woodland, M. A. Blackman, L. Haynes, T-cell immunosenescence: Lessons learned from mouse models of aging. *Trends Immunol.* **30**, 301–305 (2009).
4. K. M. Quinn, R. Palchaudhuri, C. S. Palmer, N. L. La Gruta, The clock is ticking: The impact of ageing on T cell metabolism. *Clin. Transl. Immunol.* **8**, e01091 (2019).
5. V. Gorgoulis, P. D. Adams, A. Alimonti, D. C. Bennett, O. Bischof, C. Bishop, J. Campisi, M. Collado, K. Evangelou, G. Ferbeyre, J. Gil, E. Hara, V. Krizhanovsky, D. Jurk, A. B. Maier, M. Narita, L. Niedernhofer, J. F. Passos, P. D. Robbins, C. A. Schmitt, J. Sedivy, K. Vougas, T. von Zglinicki, D. Zhou, M. Serrano, M. Demaria, Cellular senescence: Defining a path forward. *Cell* **179**, 813–827 (2019).
6. H. Chi, Regulation and function of mTOR signalling in T cell fate decisions. *Nat. Rev. Immunol.* **12**, 325–338 (2012).
7. K. Yang, S. Shrestha, H. Zeng, P. W. F. Karmaus, G. Neale, P. Vogel, D. A. Guertin, R. F. Lamb, H. Chi, T cell exit from quiescence and differentiation into Th2 cells depend on Raptor-mTORC1-mediated metabolic reprogramming. *Immunity* **39**, 1043–1056 (2013).
8. K. Yang, G. Neale, D. R. Green, W. He, H. Chi, The tumor suppressor Tsc1 enforces quiescence of naive T cells to promote immune homeostasis and function. *Nat. Immunol.* **12**, 888–897 (2011).
9. Y. Park, H. S. Jin, J. Lopez, C. Elly, G. Kim, M. Murai, M. Kronenberg, Y. C. Liu, TSC1 regulates the balance between effector and regulatory T cells. *J. Clin. Invest.* **123**, 5165–5178 (2013).
10. H. Zeng, H. Chi, mTOR signaling in the differentiation and function of regulatory and effector T cells. *Curr. Opin. Immunol.* **46**, 103–111 (2017).
11. C. L. Lucas, H. S. Kuehn, F. Zhao, J. E. Niemela, E. K. Deenick, U. Palendira, D. T. Avery, L. Moens, J. L. Cannons, M. Biancalana, J. Stoddard, W. Ouyang, D. M. Frucht, V. K. Rao, T. P. Atkinson, A. Agharahimi, A. A. Hussey, L. R. Folio, K. N. Olivier, T. A. Fleisher, S. Pittaluga, S. M. Holland, J. I. Cohen, J. B. Oliveira, S. G. Tangye, P. L. Schwartzberg, M. J. Lenardo, G. Uzel, Dominant-activating germline mutations in the gene encoding the PI(3)K catalytic subunit p110δ result in T cell senescence and human immunodeficiency. *Nat. Immunol.* **15**, 88–97 (2014).
12. A. Lanna, D. C. O. Gomes, B. Muller-Durovic, T. McDonnell, D. Escors, D. W. Gilroy, J. H. Lee, M. Karin, A. N. Akbar, A sestrin-dependent Erk-Jnk-p38 MAPK activation complex inhibits immunity during aging. *Nat. Immunol.* **18**, 354–363 (2017).
13. K. Newton, RIPK1 and RIPK3: Critical regulators of inflammation and cell death. *Trends Cell Biol.* **25**, 347–353 (2015).
14. N. Peltzer, H. Walczak, Cell death and inflammation—A vital but dangerous liaison. *Trends Immunol.* **40**, 387–402 (2019).
15. T. Tenev, K. Bianchi, M. Darding, M. Broemer, C. Langlais, F. Wallberg, A. Zachariou, J. Lopez, M. MacFarlane, K. Cain, P. Meier, The Ripoptosome, a signaling platform that assembles in response to genotoxic stress and loss of IAPs. *Mol. Cell* **43**, 432–448 (2011).
16. L. Wang, F. Du, X. Wang, TNF-alpha induces two distinct caspase-8 activation pathways. *Cell* **133**, 693–703 (2008).
17. T. B. Kang, S. H. Yang, B. Toth, A. Kovalenko, D. Wallach, Caspase-8 blocks kinase RIPK3-mediated activation of the NLRP3 inflammasome. *Immunity* **38**, 27–40 (2013).
18. J. M. Murphy, P. E. Czabotar, J. M. Hildebrand, I. S. Lucet, J. G. Zhang, S. Alvarez-Diaz, R. Lewis, N. Lalaoui, D. Metcalf, A. I. Webb, S. N. Young, L. N. Varghese, G. M. Tannahill, E. C. Hatchell, I. J. Majewski, T. Okamoto, R. C. J. Dobson, D. J. Hilton, J. J. Babon, N. A. Nicola, A. Strasser, J. Silke, W. S. Alexander, The pseudokinase MLKL mediates necroptosis via a molecular switch mechanism. *Immunity* **39**, 443–453 (2013).
19. C. P. Dillon, R. Weinlich, D. A. Rodriguez, J. G. Cripps, G. Quarato, P. Gurung, K. C. Verbist, T. L. Brewer, F. Llambi, Y. N. Gong, L. J. Janke, M. A. Kelliher, T. D. Kanneganti, D. R. Green, RIPK1 blocks early postnatal lethality mediated by caspase-8 and RIPK3. *Cell* **157**, 1189–1202 (2014).
20. W. J. Kaiser, L. P. Daley-Bauer, R. J. Thapa, P. Mandal, S. B. Berger, C. Huang, A. Sundararajan, H. Guo, L. Roback, S. H. Speck, J. Bertin, P. J. Gough, S. Balachandran, E. S. Mocarski, RIP1 suppresses innate immune necrotic as well as apoptotic cell death during mammalian parturition. *Proc. Natl. Acad. Sci. U.S.A.* **111**, 7753–7758 (2014).
21. J. A. Rickard, J. A. O'Donnell, J. M. Evans, N. Lalaoui, A. R. Poh, T. W. Rogers, J. E. Vince, K. E. Lawlor, R. L. Ninnis, H. Anderton, C. Hall, S. K. Spall, T. J. Phesse, H. E. Abud, L. H. Cengia, J. Corbin, S. Mifsud, L. di Rago, D. Metcalf, M. Ernst, G. Dewson, A. W. Roberts, W. S. Alexander, J. M. Murphy, P. G. Ekert, S. L. Masters, D. L. Vaux, B. A. Croker, M. Gerlic, J. Silke, RIPK1 regulates RIPK3-MLKL-driven systemic inflammation and emergency hematopoiesis. *Cell* **157**, 1175–1188 (2014).
22. D. Cuchet-Lourenço, D. Eletto, C. Wu, V. Plagnol, O. Papapietro, J. Curtis, L. Ceron-Gutierrez, C. M. Bacon, S. Hackett, B. Alsaleem, M. Maes, M. Gaspar, A. Alisaac, E. Goss, E. A. Idrissi, D. Siegmund, H. Wajant, D. Kumararatne, M. S. A. Zahrani, P. D. Arkwright, M. Abinun, R. Doffinger, S. Nejentsev, Biallelic RIPK1 mutations in humans cause severe immunodeficiency, arthritis, and intestinal inflammation. *Science* **361**, 810–813 (2018).
23. Y. Li, M. Führer, E. Bahrami, P. Socha, M. Klaudel-Dreszler, A. Bouzidi, Y. Liu, A. S. Lehle, T. Magg, S. Hollizeck, M. Rohlfs, R. Conca, M. Field, N. Warner, S. Mordechai, E. Shteyer, D. Turner, R. Boukari, R. Belbouab, C. Walz, M. M. Gaidt, V. Hornung, B. Baumann, U. Pannicke, E. al Idrissi, H. Ali Alghamdi, F. E. Sepulveda, M. Gil, G. de Saint Basile, M. Hönig, S. Koletzko, A. M. Muise, S. B. Snapper, K. Schwarz, C. Klein, D. Kotlarz, Human RIPK1 deficiency causes combined immunodeficiency and inflammatory bowel diseases. *Proc. Natl. Acad. Sci. U.S.A.* **116**, 970–975 (2019).
24. J. P. Dowling, Y. Cai, J. Bertin, P. J. Gough, J. Zhang, Kinase-independent function of RIP1, critical for mature T-cell survival and proliferation. *Cell Death Dis.* **7**, e2379 (2016).
25. S. Tahir, Y. Fukushima, K. Sakamoto, K. Sato, H. Fujita, J. Inoue, T. Uede, Y. Hamazaki, M. Hattori, N. Minato, A $CD153^{+}CD4^{+}$ T follicular cell population with cell-senescence features plays a crucial role in lupus pathogenesis via osteopontin production. *J. Immunol.* **194**, 5725–5735 (2015).
26. K. Shimatani, Y. Nakashima, M. Hattori, Y. Hamazaki, N. Minato, $PD\text{-}1^{+}$ memory phenotype $CD4^{+}$ T cells expressing C/EBPalpha underlie T cell immunodepression in senescence and leukemia. *Proc. Natl. Acad. Sci. U.S.A.* **106**, 15807–15812 (2009).
27. A. H. Abdelhafiz, L. Rodriguez-Manas, J. E. Morley, A. J. Sinclair, Hypoglycemia in older people—A less well recognized risk factor for frailty. *Aging Dis.* **6**, 156–167 (2015).
28. S. Dalle, L. Rossmeislova, K. Koppo, The role of inflammation in age-related sarcopenia. *Front. Physiol.* **8**, 1045 (2017).
29. F. J. H. Sorgdrager, P. J. W. Naude, I. P. Kema, E. A. Nollen, P. P. Deyn, Tryptophan metabolism in inflammaging: From biomarker to therapeutic target. *Front. Immunol.* **10**, 2565 (2019).
30. Y. Suzuki, T. Suda, K. Furuhashi, M. Suzuki, M. Fujie, D. Hahimoto, Y. Nakamura, N. Inui, H. Nakamura, K. Chida, Increased serum kynurenine/tryptophan ratio correlates with disease progression in lung cancer. *Lung Cancer* **67**, 361–365 (2010).
31. G. Weiss, T. Ganz, L. T. Goodnough, Anemia of inflammation. *Blood* **133**, 40–50 (2019).
32. R. Rossi, I. Dalle-Donne, A. Milzani, D. Giustarini, Oxidized forms of glutathione in peripheral blood as biomarkers of oxidative stress. *Clin. Chem.* **52**, 1406–1414 (2006).
33. I. Liguori, G. Russo, F. Curcio, G. Bulli, L. Aran, D. Della-Morte, G. Gargiulo, G. Testa, F. Cacciatore, D. Bonaduce, P. Abete, Oxidative stress, aging, and diseases. *Clin. Interv. Aging* **13**, 757–772 (2018).
34. J. Luo, K. Mills, S. le Cessie, R. Noordam, D. van Heemst, Ageing, age-related diseases and oxidative stress: What to do next? *Ageing Res. Rev.* **57**, 100982 (2020).
35. T. Soga, R. Baran, M. Suematsu, Y. Ueno, S. Ikeda, T. Sakurakawa, Y. Kakazu, T. Ishikawa, M. Robert, T. Nishioka, M. Tomita, Differential metabolomics reveals ophthalmic acid as an oxidative stress biomarker indicating hepatic glutathione consumption. *J. Biol. Chem.* **281**, 16768–16776 (2006).
36. J. A. Vinson, Oxidative stress in cataracts. *Pathophysiology* **13**, 151–162 (2006).
37. S. Schlesinger, S. R. Sonntag, W. Lieb, R. Maas, Asymmetric and symmetric dimethylarginine as risk markers for total mortality and cardiovascular outcomes: A systematic review and meta-analysis of prospective studies. *PLOS ONE* **11**, e0165811 (2016).
38. P. Vallance, J. Leiper, Cardiovascular biology of the asymmetric dimethylarginine:dimethylarginine dimethylaminohydrolase pathway. *Arterioscler. Thromb. Vasc. Biol.* **24**, 1023–1030 (2004).
39. A. S. Retter, Carnitine and its role in cardiovascular disease. *Heart Dis.* **1**, 108–113 (1999).
40. Z. Y. Wang, Y. Y. Liu, G. H. Liu, H. B. Lu, C. Y. Mao, l-Carnitine and heart disease. *Life Sci.* **194**, 88–97 (2018).
41. M. Scholefield, S. J. Church, J. Xu, S. Patassini, N. M. Hooper, R. D. Unwin, G. J. S. Cooper, Substantively lowered levels of pantothenic acid (vitamin B5) in several regions of the human brain in Parkinson's disease dementia. *Metabolites* **11**, 569 (2021).
42. S. Patassini, P. Begley, J. Xu, S. Church, N. Kureishy, S. Reid, H. Waldvogel, R. Faull, R. Snell, R. Unwin, G. Cooper, Cerebral vitamin B5 (D-pantothenic acid) deficiency as a potential cause of metabolic perturbation and neurodegeneration in Huntington's disease. *Metabolites* **9**, 113 (2019).
43. C. W. Tsai, S. Y. Lin, C. C. Kuo, C. C. Huang, Serum uric acid and progression of kidney disease: A longitudinal analysis and mini-review. *PLOS ONE* **12**, e0170393 (2017).
44. R. J. Johnson, T. Nakagawa, D. Jalal, L. G. Sanchez-Lozada, D. H. Kang, E. Ritz, Uric acid and chronic kidney disease: Which is chasing which? *Nephrol. Dial. Transplant.* **28**, 2221–2228 (2013).
45. N. Herranz, J. Gil, Mechanisms and functions of cellular senescence. *J. Clin. Invest.* **128**, 1238–1246 (2018).
46. G. Soto-Heredero, M. M. G. de Las Heras, E. Gabande-Rodriguez, J. Oller, M. Mittelbrunn, Glycolysis—A key player in the inflammatory response. *FEBS J.* **287**, 3350–3369 (2020).
47. G. Desdín-Micó, G. Soto-Heredero, J. F. Aranda, J. Oller, E. Carrasco, E. Gabandé-Rodríguez, E. M. Blanco, A. Alfranca, L. Cussó, M. Desco, B. Ibañez, A. R. Gortazar, P. Fernández-Marcos, M. N. Navarro, B. Hernaez, A. Alcamí, F. Baixauli, M. Mittelbrunn, T cells with dysfunctional mitochondria induce multimorbidity and premature senescence. *Science* **368**, 1371–1376 (2020).
48. L. P. Bharath, M. Agrawal, G. M. Cambridge, D. A. Nicholas, H. Hasturk, J. Liu, K. Jiang, R. Liu, Z. Guo, J. Deeney, C. M. Apovian, J. Snyder-Cappione, G. S. Hawk, R. M. Fleeman, R. M. F. Pihl,

K. Thompson, A. C. Belkina, L. Cui, E. A. Proctor, P. A. Kern, B. S. Nikolajczyk, Metformin enhances autophagy and normalizes mitochondrial function to alleviate aging-associated inflammation. *Cell Metab.* **32**, 44–55.e6 (2020).

49. J. Suzuki, T. Yamada, K. Inoue, S. Nabe, M. Kuwahara, N. Takemori, A. Takemori, S. Matsuda, M. Kanoh, Y. Imai, M. Yasukawa, M. Yamashita, The tumor suppressor menin prevents effector CD8 T-cell dysfunction by targeting mTORC1-dependent metabolic activation. *Nat. Commun.* **9**, 3296 (2018).
50. A. Najafov, H. S. Luu, A. K. Mookhtiar, L. Mifflin, H.-G. Xia, P. P. Amin, A. Ordureau, H. Wang, J. Yuan, RIPK1 promotes energy sensing by the mTORC1 pathway. *Mol. Cell* **81**, 370–385.e7 (2021).
51. X. Mei, Y. Guo, Z. Xie, Y. Zhong, X. Wu, D. Xu, Y. Li, N. Liu, Z. J. Zhu, RIPK1 regulates starvation resistance by modulating aspartate catabolism. *Nat. Commun.* **12**, 6144 (2021).
52. A. Takahashi, T. M. Loo, R. Okada, F. Kamachi, Y. Watanabe, M. Wakita, S. Watanabe, S. Kawamoto, K. Miyata, G. N. Barber, N. Ohtani, E. Hara, Downregulation of cytoplasmic DNases is implicated in cytoplasmic DNA accumulation and SASP in senescent cells. *Nat. Commun.* **9**, 1249 (2018).
53. Y. Wang, Z. Fu, X. Li, Y. Liang, S. Pei, S. Hao, Q. Zhu, T. Yu, Y. Pei, J. Yuan, J. Ye, J. Fu, J. Xu, J. Hong, R. Yang, H. Hou, X. Huang, C. Peng, M. Zheng, Y. Xiao, Cytoplasmic DNA sensing by KU complex in aged $CD4^+$ T cell potentiates T cell activation and aging-related autoimmune inflammation. *Immunity* **54**, 632–647.e9 (2021).
54. H. J. Chun, L. Zheng, M. Ahmad, J. Wang, C. K. Speirs, R. M. Siegel, J. K. Dale, J. Puck, J. Davis, C. G. Hall, S. Skoda-Smith, T. P. Atkinson, S. E. Straus, M. J. Lenardo, Pleiotropic defects in lymphocyte activation caused by caspase-8 mutations lead to human immunodeficiency. *Nature* **419**, 395–399 (2002).
55. L. Salmena, B. Lemmers, A. Hakem, E. Matysiak-Zablocki, K. Murakami, P. Y. B. Au, D. M. Berry, L. Tamblyn, A. Shehabeldin, E. Migon, A. Wakeham, D. Bouchard, W. C. Yeh, J. C. McGlade, P. S. Ohashi, R. Hakem, Essential role for caspase 8 in T-cell homeostasis and T-cell-mediated immunity. *Genes Dev.* **17**, 883–895 (2003).
56. B. K. Kennedy, D. W. Lamming, The mechanistic target of rapamycin: The grand ConducTOR of metabolism and aging. *Cell Metab.* **23**, 990–1003 (2016).
57. S. Robida-Stubbs, K. Glover-Cutter, D. W. Lamming, M. Mizunuma, S. D. Narasimhan, E. Neumann-Haefelin, D. M. Sabatini, T. K. Blackwell, TOR signaling and rapamycin influence longevity by regulating SKN-1/Nrf and DAF-16/FoxO. *Cell Metab.* **15**, 713–724 (2012).
58. J. B. Mannick, G. D. Giudice, M. Lattanzi, N. M. Valiante, J. Praestgaard, B. Huang, M. A. Lonetto, H. T. Maecker, J. Kovarik, S. Carson, D. J. Glass, L. B. Klickstein, mTOR inhibition improves immune function in the elderly. *Sci. Transl. Med.* **6**, 268ra179 (2014).
59. U. Ozcan, L. Ozcan, E. Yilmaz, K. Düvel, M. Sahin, B. D. Manning, G. S. Hotamisligil, Loss of the tuberous sclerosis complex tumor suppressors triggers the unfolded protein response to regulate insulin signaling and apoptosis. *Mol. Cell* **29**, 541–551 (2008).
60. D. W. Huang, B. T. Sherman, R. A. Lempicki, Systematic and integrative analysis of large gene lists using DAVID bioinformatics resources. *Nat. Protoc.* **4**, 44–57 (2009).

Acknowledgments: We thank E. Miyauchi, H. Ishigame, H. Iseki, K. Moro, and S. Matsuda for discussions and experimental help; M. Sakuma and K. Otaki for technical support; P. Burrows for helpful comments on the manuscript; and M. Yoshioka for secretarial assistance. **Funding:** This work was supported by a Grant-in-Aid for Scientific Research from the Japan Society for the Promotion of Science KAKENHI (grant number 21K07087 for T.I.) and the Takeda Science Foundation (E0120034). **Author contributions:** T.I. designed the study, performed experiments, and wrote the manuscript. M.U. and N.Y. performed the experiments. Y.M., M.M., and T.Sas. provided technical help. M.P. provided KO mice. T.Sai. supervised the study and wrote the manuscript. **Competing interests:** The authors declare that they have no competing interests. **Data and materials availability:** All data needed to evaluate the conclusions in the paper are present in the paper and/or the Supplementary Materials. The *Ripk1*$^{fl/fl}$ and *Ripk1*$^{D138N/D138N}$ mice can be provided by M.P. (University of Cologne) pending scientific review and a completed material transfer agreement. Requests for the *Ripk1*$^{fl/fl}$ and *Ripk1*$^{D138N/D138N}$ mice should be submitted to M.P. (University of Cologne). RNA-seq data can be found publicly available on the NCBI GEO website under accession number GSE197232.

Submitted 22 June 2022
Accepted 22 December 2022
Published 25 January 2023
10.1126/sciadv.add6097